Lung Cancer 213 (2026) 108939

Contents lists available at ScienceDirect

Lung Cancer

journal homepage: www.elsevier.com/locate/lungcan

Research Paper

Targeting HGF/MET and CXCL1/CXCR2 axes bypasses resistance to KRAS^{G12C} inhibitors in NSCLC

A. Cavazzoni [a,1], M. Pagano Mariano [a,b,1], A. Palladini [c,d], G. Digiacomo [a], S. La Monica [a], M. Bonelli [a], M. Galetti [e], I. Pace [b], R. Roncarati [b,f], E. Giovannetti [g,h], P. Aretini [g], R. Minari [i], M. Treccani [j], M. Pluchino [i], C.A. Lagrasta [a], S. Angelicola [k], G. Mazzaschi [i], P. Bordi [i], F. Gelsomino [k], F. Agustoni [d,l], P.G. Petronini [a], M. Tiseo [a,i,*], M. Ferracin [b,k,2], R. Alfieri [a,2,*]

[a] Department of Medicine and Surgery, University of Parma, Parma 43126, Italy
[b] Department of Medical and Surgical Sciences, University of Bologna, Bologna 40126, Italy
[c] Department of Molecular Medicine, University of Pavia, Pavia 27100, Italy
[d] Medical Oncology Division, Fondazione IRCCS Policlinico San Matteo, Pavia 27100, Italy
[e] Department of Occupational and Environmental Medicine, Epidemiology and Hygiene, INAIL-Italian Workers' Compensation Authority, Monte Porzio Catone, Rome 00078, Italy
[f] CNR Institute of Molecular Genetics "Luigi Luca Cavalli-Sforza", Unit of Bologna, Bologna 40136, Italy
[g] Department of Medical Oncology, Cancer Center Amsterdam, Amsterdam UMC, VU University, Amsterdam 1081 HV, the Netherlands
[h] Cancer Pharmacology Laboratory, Fondazione Pisana per la Scienza, Pisa 56017, Italy
[i] Medical Oncology Unit, University Hospital of Parma, Parma 43126, Italy
[j] Department of Food and Drug, University of Parma, Parma 43125, Italy
[k] Medical Oncology, IRCCS Azienda Ospedaliero-Universitaria di Bologna, Bologna 40126, Italy
[l] Department of Internal Medicine and Medical Therapy, University of Pavia, Pavia 27100, Italy

ARTICLE INFO

Keywords:
NSCLC
KRAS
Sotorasib
Adagrasib
Resistance

ABSTRACT

Background: Resistance to KRAS^{G12C} inhibitors sotorasib and adagrasib, approved for KRAS^{G12C}-mutant advanced Non-Small Cell Lung Cancer (NSCLC), involves multiple subclonal events, raising significant concerns about overcoming the resistant phenotype. Cytokines, chemokines, and growth factors are key mediators of drug resistance and targeting their signaling pathways is an emerging strategy in cancer therapy.

Methods: We generated cell clones from KRAS^{G12C}-mutated NSCLC cells treated with KRAS inhibitors and cell cultures from a sotorasib-resistant patient-derived xenograft (PDX). Gene mutations and changes in gene expression were evaluated using NGS, RNAseq. The mRNA and protein levels encoded by the Hepatocyte Growth Factor (HGF) and CXCL1 genes were quantified using RT-PCR and ELISA assay. The effect of drug combination was obtained by the Sulforhodamine-B assay and analyzed by Combenefit Software. Cell death was detected by Annexin-V assay. Cell signaling and epithelial-to-mesenchymal transition were evaluated by Western blotting.

Results: NSCLC cell clones and PDX cell cultures with acquired and intrinsic resistance to KRAS^{G12C} inhibitors exhibited elevated levels of CXCL1 and HGF expression and secretion, with activation of CXCR2 and c-MET signalling pathways. The combination of CXCR2 and c-MET inhibitors led to synergistic inhibition of cell growth and reduced cell viability by inhibiting the ERK1/2 and AKT signalling pathways. This combination also reversed EMT and induced apoptosis in sotorasib- and adagrasib-resistant clones, regardless of the genetic alterations responsible for resistance.

Conclusions: CXCL1/CXCR2 and HGF/c-MET may represent compensatory pathways that sustain proliferation and survival in resistance to KRAS^{G12C} inhibitors. The simultaneous blockade of these signals may offer a novel strategy for bypassing resistance.

* Corresponding author.
E-mail addresses: marcello.tiseo@unipr.it (M. Tiseo), roberta.alfieri@unipr.it (R. Alfieri).
[1] Cavazzoni A. and Pagano Mariano M. have equally contributed.
[2] Co-last authors.

https://doi.org/10.1016/j.lungcan.2026.108939
Received 13 November 2025; Received in revised form 22 December 2025; Accepted 20 January 2026
Available online 21 January 2026

1. Introduction

Non-Small Cell Lung Cancer (NSCLC) is the most prevalent form of lung cancer, representing approximately 85 % of all lung cancer cases. Patients harboring driver gene alterations such as EGFR, ALK, ROS1, RET, BRAF, MET, NTRK and HER2 account for 30 % of NSCLC cases and currently received targeted agents in different treatment setting [1]. For the remainder, immune checkpoint inhibitors (ICIs) alone or combined with a platinum-based regimen is the best option. [2].

KRAS is the most frequently mutated oncogene in NSCLC, with a frequency of approximately 30 % [3,4]. It encodes a protein that functions as a GTPase enzyme that cycles between an active state (GTP-bound) and an inactive state (GDP-bound). The KRAS mutations favor the active form, inhibiting its intrinsic GTPase activity and causing continuously on-signals of the mitogen-activated protein kinases (MAPK/ERK) downstream pathway. The $KRAS^{G12C}$ mutation is particularly common in NSCLC, accounting for approximately 13 % of cases [5].

The development of $KRAS^{G12C}$ inhibitors represented a significant breakthrough in the treatment of NSCLC. Two recent pharmaceutical agents, sotorasib (AMG 510) [6] and adagrasib (MRTX849) [7] have been authorized for the treatment of advanced NSCLC patients carrying $KRAS^{G12C}$ mutation who have previously undergone at least one systemic therapy. In the phase III clinical trial CodeBreaK 200, sotorasib was superior to docetaxel, in terms of progression-free survival (PFS) and objective response rate (ORR) for previously treated $KRAS^{G12C}$ mutated NSCLC patients [8]. Adagrasib, received approval in December 2022 based on the results from Krystal-1 clinical trial [7]. Subsequently, superiority in terms of PFS and ORR was also demonstrated for this agent in the phase III Krystal-12 trial [9]. These trials demonstrated similar objective response rates (around 30–40 %) and PFS (around 5–6 months) in previously treated NSCLC patients. Ongoing clinical trials are evaluating the efficacy and safety of these drugs across different settings and combined with other therapies (such as chemotherapy and/or ICIs).

As with many cancer therapies, sotorasib and adagrasib may lose efficacy over time as cancer cells develop resistance [10]. The mechanisms behind this resistance are diverse and complex, and many are not fully understood, yet. They can arise through processes that are dependent or independent on KRAS itself. Reported KRAS-dependent mechanisms include the emergence of alternative KRAS mutations, activation of other RAS isoforms, and upregulation of KRAS expression [11], whereas KRAS-independent included activation of alternative signaling pathways [11] or histologic transformation to small-cell carcinoma.

Studies have demonstrated that resistance to $KRAS^{G12C}$ inhibitors can be highly heterogenous with multiple subclonal events occurring within the same patient during treatment [11,12]. The presence of heterogeneity, in conjunction with subclonality, poses a significant challenge in overcoming the resistant phenotype. To this end, exploring and implementing novel approaches that expand beyond genetic alterations is necessary.

Cytokines, chemokines, and growth factors can influence the behaviour of cancer cells and play complex roles in cancer progression, promoting growth, survival, metastasis, and therefore altering the effectiveness of cancer therapies [13–15]. They are critical components of the tumor microenvironment and modulate how cancer cells interact with surrounding stromal and immune cells. They may be released from tumor cells as well as from the microenvironment and, in some cases, are detected in human blood, representing a potential biomarker for treatment resistance [16].

CXCL1 is a pro-inflammatory chemokine, frequently elevated in tumors. CXCL1 has a high affinity for CXCR2, a G-protein-coupled receptor that binds multiple chemokines. In lung adenocarcinoma it has been identified as a poor prognostic marker associated with tumor metastasis and progression [17,18]. The CXCL1/CXCR2 axis regulates cell proliferation, apoptosis, senescence and epithelial-to-mesenchymal transition (EMT) in various cancer cells by activating pathways including PI3K/AKT, p38/ERK, and STAT signaling [19,20]. Most recently, this axis has been linked to drug resistance [21]. For example, elevated expression levels of CXCL1 and CXCL5 are increased in colon cancer cell lines harboring KRAS or BRAF mutations and resistant to cetuximab [22].

The activation of the HGF/MET axis triggers a range of biological responses critical for tumor progression including increasing migration, proliferation, survival, and angiogenesis [23].

c-MET alterations in NSCLC encompass dysregulation mechanisms like MET exon 14 skipping mutations (2–4 % prevalence), MET amplification (1–6 %), MET fusions (0.2–0.3 %), and c-MET overexpression (20–50 %, higher in adenocarcinomas), all contributing to oncogenic signalling dysregulation driving tumor progression, invasion and metastasis [24,25].

HGF/MET downstream signalling acts as a bypass mechanism in cancer cell significantly contributing to resistance against various targeted therapies. Notably, HGF/MET activation has been involved in resistance to EGFR tyrosine kinase inhibitors (TKIs) and to RET inhibitors in NSCLC, cetuximab in colon rectal cancer, trastuzumab in breast cancer, and BRAF inhibitors in melanoma [26–29]. MET is a driver of RAS pathway through SOS-dependent activation, but MET can also independently activate PI3K-AKT and JAK-STAT3 signalling, thus sustaining resistance to KRAS inhibitors [30,31].

Amplification of *MET* gene, confirmed by FISH, was indeed reported as mechanism of resistance to sotorasib in clones derived from the sotorasib-sensitive $KRAS^{G12C}$ NSCLC H23 cell line after chronic exposure with the drug. Loss of MET function through silencing or by treatment with the MET inhibitor crizotinib restored sotorasib sensitivity both in vitro and in vivo by suppressing ERK and AKT activity [31].

In the present study, we demonstrated that NSCLC clones with acquired resistance to sotorasib and adagrasib displayed higher levels and secretion of CXCL1 and HGF associated with increased expression of their respective receptors CXCR2 and MET without gene amplification. ERK1/2 and AKT signalling promote survival and proliferation in drug-resistant clones. This is also linked to EMT, which increases the expression of mesenchymal markers such as N-cadherin and Slug, while decreasing the expression of E-cadherin, thereby enhancing migration. Interestingly, cell cultures established from the patient-derived xenograft (PDX) of a patient experiencing primary resistance to sotorasib, with multiple genetic alterations associated with resistance, presented elevated mRNA and protein levels of CXCL1 and HGF. The combination of the MET inhibitor crizotinib, with the selective competitive CXCR2 antagonist SB225002, synergistically inhibited cell proliferation and promoted apoptosis in these preclinical models of $KRAS^{G12C}$ inhibitors resistance. These results suggest that targeting both the HGF/MET and CXCL1/CXCR2 axes is a promising strategy to bypass resistance in $KRAS^{G12C}$-mutant NSCLC.

2. Material and methods

2.1. Drug treatments

Sotorasib, adagrasib, crizotinib, and SB225002 (N-(2-hydroxy-4-nitrophenyl)-N'-(2-bromophenyl)urea) were purchased from Selleckchem (Houston, TX). All drugs were dissolved in DMSO, which never exceeded 0.1 % (v/v) in the treatment solutions; equal amounts of the solvent were added to control cells.

2.2. Cell lines and culture conditions

A549 ($KRAS^{G12S}$), Calu-1, H358, and H23 ($KRAS^{G12C}$) NSCLC cells were from American Type Cell Culture (ATCC) and were cultured as recommended in RPMI medium with 100 U/ml penicillin and 100 μg/ml streptomycin and incubated at 37 °C in a humidified atmosphere of 5 % CO_2 in the air. H23-resistant cells were generated by parental cells by chronic exposure to sotorasib and adagrasib in a period of 4–6 months.

Resistant clones were maintained with 1 μM sotorasib (clones S1 and S2) and 0.5 μM adagrasib (clones A1 and A2).

2.3. Clinical history of the patient and establishment of PDX-derived cell cultures

A 48-year-old female, smoker patient was diagnosed with stage IVB NSCLC, carrying a $KRAS^{G12C}$ mutation. After two prior treatment lines, including pembrolizumab combined with pemetrexed and carboplatin followed by docetaxel, the patient received sotorasib 960 mg daily, obtaining progressive disease (PD) as best response. Tumor was sampled and collected at the time of PD on sotorasib and after the patient gave her informed consent. The protocol was approved by the Ethics Committee Center Emilia-Romagna Region, Italy (GR-2018–12368031). Human biological samples and metadata including relevant clinical data were de-identified before being shared between laboratories involved in this study to protect patient privacy and respect the ethical standards. All animal procedures were performed in accordance with European directive 2010/63/UE and Italian Law (No. DL26/2014). Experimental protocols were reviewed and approved by the institutional animal care and use committee of the University of Bologna and by the Italian Ministry of Health with letter 32/2020-PR.

ADK-35a and ADK-35b cell cultures were derived from the tumor mass of the first passage patient-derived xenograft (PDX) established from the patient. Briefly, a fragment of lung metastasis obtained from the patient (diameter of around 3–4 mm) was implanted into the interscapular fat pad of a BALB/c Rag2 −/−; Il2rg −/− (BRG) immunodeficient mice [32]. After euthanizing the BRG mouse used for PDX establishment, the tumor mass was excised and collected in cold PBS. The tumor mass was then dissected, and the resulting fragments were placed into 25 cm^2 PRIMARIA tissue culture flasks (Corning). The cell lines were established in MammoCult medium (STEMCELL Technologies) supplemented with 1 % fetal bovine serum (FBS, Thermo Fisher Scientific), 100 U/mL penicillin, and 100 μg/mL streptomycin (Thermo Fisher Scientific) and were subsequently maintained in standard cell culture conditions.

2.4. Genomic analyses

Next generation sequencing analyses were performed at different depths and in different samples to better elucidate potential resistance mechanisms.

Targeted sequence analysis.

Next Generation Sequencing was performed using the TruSight Oncology 500 (Illumina) on the NextSeq550 platform (Illumina®, San Diego, CA) according to the manufacturer's protocol. Genomic DNA and RNA were extracted using the QIAamp DNA Blood Mini Kit (Qiagen®, Valencia, CA, USA) and quantified with QuantiFluor® dsDNA and QuantiFluor® RNA System (Promega).

Whole Genome Sequencing (WGS).

According to the manufacturer's instructions, genomic DNA was extracted using the Qiamp DNA mini-Kit (Qiagen). DNA libraries were prepared by Eurofins Genomics (Germany) using Illumina technology with paired-end sequencing (2x150bp reads), generating an average of 90 GB of raw data per sample. Raw sequencing data were preprocessed to obtain clean reads for downstream analysis. Good quality reads were mapped against the human reference genome sequence (hg19 release) using BWA MEM version 0.7.12 [33], within the Sentieon framework version 202308.03. The SNP and InDel calling were also conducted using Sentieon's DNAscope version 0.5.

2.5. Bioinformatics analysis

After variant calling and annotation, genetic data underwent quality controls using bcftools version 1.17 [34]. Variants flagged as PASS and with a read depth (DP) > 10 were retained. Additionally, variants shared between parental and each treated cell line or unique to each treated cell line were selected using vcftools version 0.1.17 [35]. Finally, variants with a variant allele frequency (VAF) > 0.05 and predicted to have a nonsynonymous effect were kept for further analysis. Genes functionality was assessed using the Search Tool for the Retrieval of Interacting Genes/Proteins (STRING) database version 12.0 [36] with parameters set to include the full network type, all the available interaction sources ("Textmining", "Experiments", "Databases", "Co-expression", "Neighborhood", "Gene Fusion", and "Co-occurrence"), and a minimum required interaction confidence score of 0.400 (medium confidence). STRING enrichment analysis was performed on the Gene Ontology [37,38] database, applying the Benjamini-Hochberg procedure to control the false discovery rate (FDR) at a threshold of < 0.05.

2.6. Rna sequencing and analysis

The transcriptomics design included 8 samples, each processed in duplicate to ensure robustness.

Total RNA was extracted using the miRNeasy Mini Kit (Qiagen, Venlo, The Netherlands), following the manufacturer's total RNA extraction protocol. RNA quality was assessed with Bioanalyzer and samples with RNA integrity number (RIN) greater than 8 were used for library preparation. RNA-Seq libraries were generated using the Qiagen QIAseq FastSelect RNA Removal Kit and the Qiagen QIAseq Stranded Total RNA Library Kit, strictly following the manufacturer's instructions. Briefly, 500 ng of total RNA was used as the input for each sample. The protocol included a first step of Ribosomal RNA (rRNA) removal obtained using Qiagen FastSelect kits after a heat fragmentation step. Subsequently, first-strand synthesis using reverse transcription, second strand synthesis, end-repair, A-tailing, and adapter ligation steps were performed as detailed in the kit manual.

The resulting DNA libraries were evaluated for quality and quantity using the Agilent TapeStation system using the Agilent High Sensitivity DNA D1000 kit. Equimolar pooling of 16 libraries was performed prior to sequencing. Sequencing was conducted on the Illumina NextSeq 500 platform using a high-output flow cell and the NextSeq High Output kit v2.5. Paired-end sequencing was performed with read lengths of 75 nucleotides in each direction, generating a combined read length of 150 nucleotides per fragment indicated for gene expression analysis.

Raw sequencing data were processed to produce FASTQ files, which were subsequently trimmed and aligned to the human reference genome (hg 19) using the STAR aligner version 2.7.10a for transcript mapping and counting. Gene-level raw counts were normalized using DESeq2.

Differential expression between groups was assessed using a 2-fold change threshold combined with a moderated *t*-test. To control false positives arising from multiple testing, p-values were adjusted using the Benjamini-Hochberg procedure to control the false discovery rate (FDR) at 5 %. All statistical analyses were performed using GeneSpring GX software.

A Gene Set Enrichment Analysis (GSEA) was performed using the HALLMARK gene sets from the MSigDB (Molecular Signatures Database) through the clusterProfiler package in R.

2.7. Quantitative Real-Time PCR

Total RNA was isolated using the RNAeasy Mini Kit (Qiagen, Venlo, The Netherlands) and quantitative real-time polymerase chain reaction (PCR) was performed as previously described [39]. Primers for HGF (QT00065695) and CXCL1 (QT00199752) were purchased from Qiagen. The housekeeping genes Actin and GAPDH were also obtained from Qiagen (QT01680476 and QT00079247).

2.8. Fluorescence in Situ Hybridization

Cells were fixed with 4 % paraformaldehyde, cytospinned and pretreated in SSC 2x buffer for 30 min at 80 °C. MET amplification was

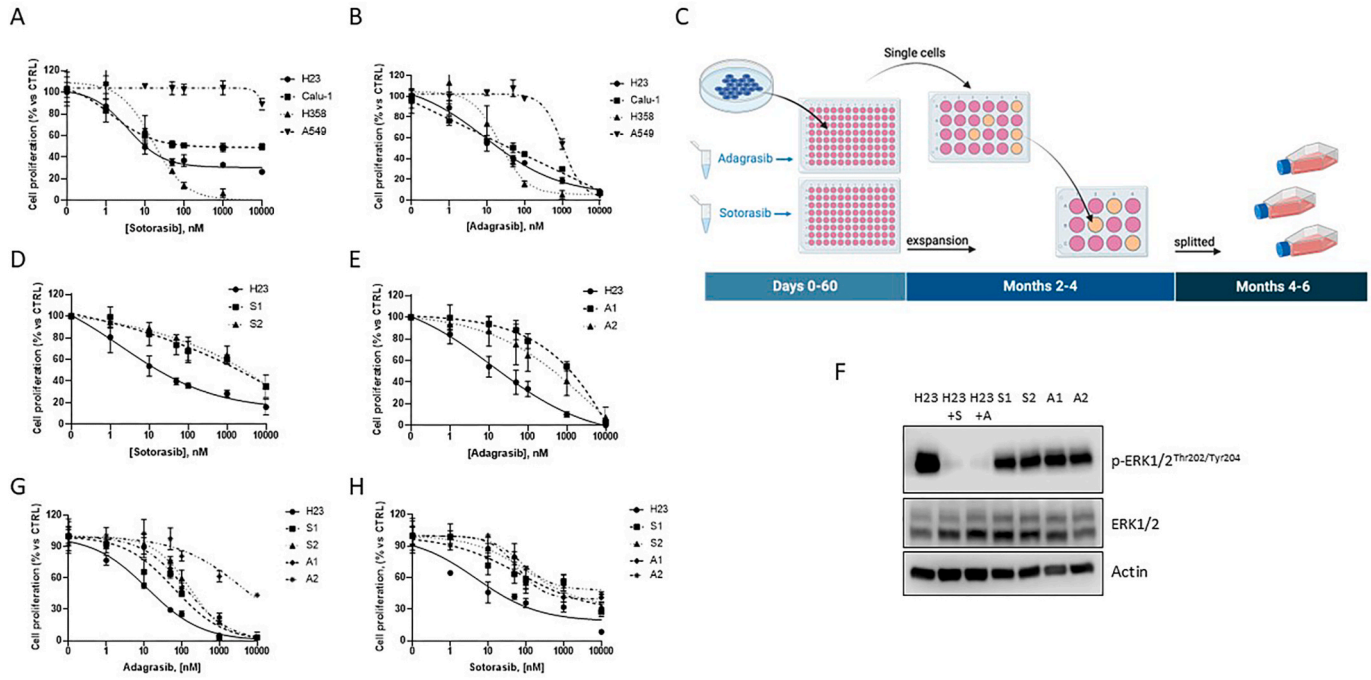

Fig. 1. Generation of sotorasib and adagrasib resistant clones. (A-B) NSCLC cells H23, Calu-1, H358 and A549 were treated with increasing doses of sotorasib (A) or adagrasib (B) for 72 h and cell proliferation was assessed by SRB assay and expressed as percent vs untreated (CTRL) cells. (C) Schematic representation of timing for isolation of resistant clones. (D-E) H23 parental cells and S1, S2, A1 and A2 clones were treated with increasing doses of sotorasib (D) or adagrasib (E), respectively and after 72 h cell proliferation was evaluated by SRB assay and expressed as percent vs untreated (CTRL) cells. (F) The level of ERK1/2 phosphorylation was evaluated in H23 cells, in the absence or the presence of 1 μM sotorasib or 0.5 μM adagrasib for 24 h and in the S1, S2, A1, and A2 clones at the same drug dosage. (G-H) All the resistant clones were treated with increasing doses of both $KRAS^{G12C}$ inhibitors; after 72 h cell proliferation was assessed by SRB assay and the results were expressed as percent vs. untreated (CTRL) cells for both adagrasib (G) and sotorasib (H). A, B, F, G, and H are representative of two independent experiments; D and E are the average of three independent experiments.

evaluated using specific a specific probe (Leica Bosystems) and following manufacturer's instructions. MET was considered amplified when 5 MET gene copies are detected in ≥ 40 % of the cells. Samples were viewed at 1000X magnification, employing a Nikon Ni-U fluorescence microscope (Nikon Corporation, Tokyo, Japan) equipped with an optic fiber. Images were acquired by the software NIS-Elements AR 5.01.00.

2.9. Measurement of HGF and CXCL1 production

The ELISA Quantikine Human Immunoassay kits (R&D System, Minneapolis, MN, USA) were used to quantify human HGF and CXCL1 in cell culture media, following the manufacturer's instructions.

2.10. Flow cytometry

To determine membrane expression of CXCR2, cells were harvested and incubated with either phycoerythrin (PE)-conjugated mouse IgG1 isotype control or PE-conjugated anti-human CXCR2 antibody (BD Biosciences, San Jose, CA, USA). The quantification was performed using a Beckman FC500 flow cytometer and data were analyzed with FCS express software (De Novo software, Pasadena, CA, USA).

2.11. Cell viability and apoptosis assays

Cell viability was measured using the SRB (sulforhodamine B) assay. Briefly, 3×10^3 cells were seeded into 96-well plates. After 72 h treatment, cells were fixed with 50 % ice-cold trichloroacetic acid (TCA) and stained with 0.4 % SRB solution in 1 % acetic acid. Tris(hydroxymethyl) aminomethane solution pH 8.8 was added to solubilize SRB, and the optical density (OD) was measured at 490 nm. Drug-induced apoptotic effect was evaluated using the eBioscience Annexin C-FITC Apoptosis Detection Kit (Invitrogen CN: BMS500FI-100) according to the manufacturer's instructions. Flow cytometry analysis was performed using the Cytoflex cytometer (Beckman Coulter), and data was processed by CytExpert software. Cell death was quantified as the combined percentage of Annexin V positive and propidium iodide positive cells.

2.12. Cell migration and Spheroid generation

The migration assay was carried out using 6.5 mm Transwell® with 8.0 μm Pore Polycarbonate Membrane Insert (Corning, NY, USA) as previously described [39]. Briefly, 10^5 cells were loaded in the upper wells. After 16 h, cells that have migrated through the PET membranes were fixed with 100 % methanol, stained with hematoxylin and counted under a Phase contrast microscope.

To generate 3D spheroids, U-shaped 96-well plates were covered with 80 μL of warm 1.5 % agarose in PBS. After 30 min 1.5 x 10^3 cells were added in 80 μL of medium and after 24 h drugs were added to the medium. Pictures of spheroids were taken every 5 days using Nikon Eclipse E400 Microscope with digital Net camera.

2.13. Evaluation of the effects of drug combinations

To evaluate the combined effects of the drugs, the Combenefit software was used. This software employs a dose-matrix approach to predict potential synergy, antagonism, or additivity between drugs [40]. BLISS model is a statistical model used to evaluate drug combination synergy by comparing observed effects to expected additive outcomes from single agents, with positive excess indicating synergy. HSA model assessed combination efficacy by contrasting the mixture's effect against the strongest single drug response.

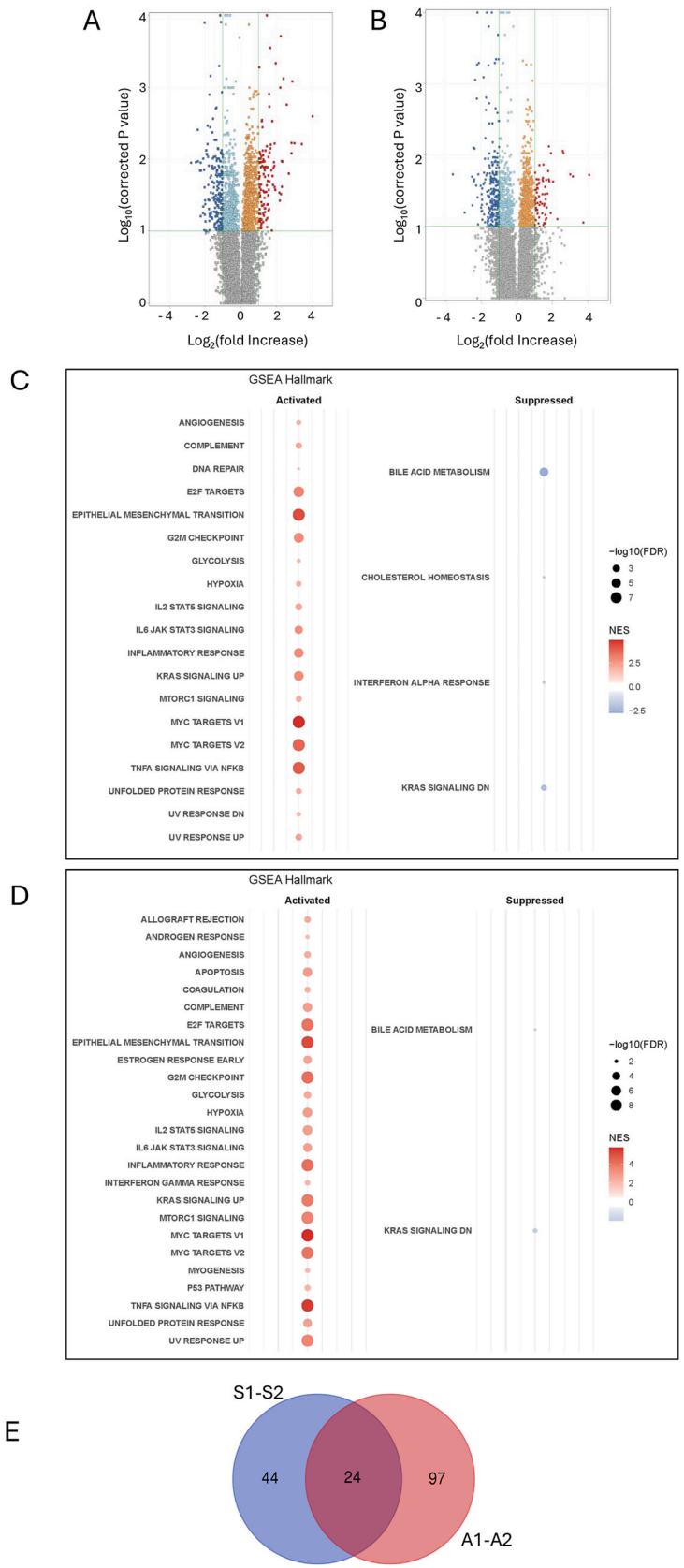

Fig. 2. RNAseq analysis of KRAS^{G12C} resistant clones. (A-B) Volcano plot of sotorasib (A) or adagrasib (B) resistant clones vs H23 cells treated with sotorasib or adagrasib 1 and 0.5 μM, respectively. (C-D) Gene Set Enrichment Analysis (GSEA) was performed to identify the main biological pathways activated or suppressed in sotorasib (C) and adagrasib-resistant clones (D). (E) Venn diagram reveals overlapping upregulated genes amongst sotorasib and adagrasib-resistant clones.

2.14. Western blotting

Procedures for protein extraction, solubilization, and protein analysis by 1-D PAGE were previously described. Antibodies against p-ERK1/2 (Thr202/Tyr204), p-MET (Tyr1234/1235), p-AKT (Ser473), p-STAT3 (Ser705), p-IκBα (Ser32), ERK1/2, AKT, c-MET, STAT3, IκBα, E-cadherin, Snail, Slug, vimentin and HRP-conjugated secondary antibodies were obtained from Cell Signaling Technology (Danvers, MA. USA); Actin was from Invitrogen (Thermo Fisher, MA, USA); N-cadherin was from Ab Clonal (Woburn, MA, USA); the chemiluminescence system (Immobilion^{TM} Western Chemiluminescent HRP Substrate) was from Millipore (Temecula, CA, USA). Reagents for electrophoresis and blotting analysis were supplied from BIO-RAD (Hercules, CA, USA). The chemiluminescent signal was acquired using the C-DiGit R Blot Scanner.

2.15. Digital live imaging

The digital holographic microscope HoloMonitor® M4 was used to monitor cell growth and morphology in culture. Cells were seeded into a 96-well lumox® plate (Sarstedt) at a density of 3×10^3 cells. After allowing the cell adhesion, HoloLids (71130, Phase Holographic Imaging AB), were replaced on the plate lid, and the well plate was then immediately positioned on the HoloMonitor® M4, inside a humidified incubator maintained at 37 °C and 5 % CO_2. Cell images were captured at time interval of 4 h. At the end of the experiment, M4 Studio tracking software 2.6.2 was used to analyze the data.

2.16. Statistical analysis

Statistical analyses were carried out using GraphPad Prism version 8.0 software (GraphPad Software, San Diego, CA). Comparisons were performed by the two-tailed Student's *t*-test, and the ANOVA test and p-values are indicated where appropriate.

3. Results

3.1. Generation of H23-resistant clones to KRAS^{G12C} inhibitors

The KRAS-mutated NSCLC cell lines H358, H23 and Calu-1, which express KRAS^{G12C}, as well as A549, which expresses KRAS^{G12S}, were treated with the KRAS^{G12C} inhibitors sotorasib and adagrasib. As expected, (Fig. 1A-B), cancer cells harboring the KRAS^{G12C} mutation were more responsive to treatment with both sotorasib and adagrasib (IC_{50} in the low nanomolar range) compared to the A549 cell line ($IC_{50} < 10$ and 1 μM for sotorasib and adagrasib respectively).

We generated resistant clones by treating sensitive H23 cells (IC_{50} = 32 and 14 nM for sotorasib and adagrasib, respectively) with increasing drug concentrations. After four months for sotorasib and six months for adagrasib (Fig. 1C), we isolated and expanded four independent clones from single cells: S1 and S2 resistant to sotorasib (IC_{50} = 3.4 and 2.7 μM, respectively) (Fig. 1D), and A1 and A2 resistant to adagrasib (IC_{50} = 0.95 and 0.76 μM, respectively) (Fig. 1E) which proliferated freely in the presence of 1 μM sotorasib (clones S1 and S2) and 0.5 μM adagrasib (clones A1 and A2). We then analysed the activation of the KRAS effector ERK1/2 by immunoblotting. Sotorasib or adagrasib treatment strongly decreased ERK1/2 phosphorylation in H23 cells, while all the resistant clones maintained ERK1/2 activation despite drug treatments (Fig. 1F). It is noteworthy that sotorasib resistance is associated with adagrasib resistance (Fig. 1G). Similarly, A1 and A2 demonstrated resistance to sotorasib (Fig. 1H), confirming cross-resistance.

3.2. Evaluation of genetic alterations and analysis of RNA transcriptome in resistant clones over parental cells

An NGS analysis on approximately 500 genes was performed to identify potential genetic alterations responsible for resistance to KRAS inhibitors.

The resistant clones (S1, S2, A1 and A2) retained the KRAS^{G12C} mutation, exhibiting an allelic frequency that was analogous to that of the H23 parental cells (80.8 %, 75.7 %, 76 % and 75 % versus 75.1 %). No secondary KRAS mutations were reported. Aiming at the identification of candidate variants, we obtained 23 variants (Table S1) across 13 chromosomes presented in at least one cell clone and absent in the parental cells. Among these, the most abundant comprised 8 missense, 7 intronic, and 3 splice region variants. Only the 7 missense variants (underlined in Table S1) were further taken into consideration, according to their biological meaning. All the selected variants were heterozygotes in all the clones. Clones S1 and A1 were characterized by the presence of 3 variants each, clone S2 by 2 variants, while clone A2 displayed only a single variant. No variants were shared between the four clones, and only a single variant located on gene MSH6 (NM_000179.2c.2137G > C; p.(Asp713His)) was shared between three of them (S1, S2, and A1), with a higher VAF in the sotorasib clones (VAF = 14 % and VAF = 13 %) than in the adagrasib clone (VAF = 6 %). Computational functional analysis identified 7 nodes (genes) connected by 6 edges, with an average node degree of 1.71 and a protein–protein interaction (PPI) enrichment p-value of 0.000101 (not shown). However, no significant functional terms were identified in any database.

Since this analysis did not show any clear genetic alteration involved in resistance to KRAS inhibitors, to further dissect molecular features of resistant clones, we performed a RNAseq analysis to compare the expression levels of mRNAs between resistant clones maintained with sotorasib or adagrasib and H23-treated parental cells. We identified 320 and 306 genes differently expressed in sotorasib and adagrasib-resistant clones, over H23-treated cells, respectively (Fig. 2A-B). A GSEA was performed to identify the main biological pathways activated or suppressed in sotorasib and adagrasib-resistant clones (Fig. 2C-D). The results were visualized using a bubble plot, which displays for each pathway the enrichment level (NES) and statistical significance (FDR).

In both sotorasib and adagrasib resistant clones, EMT, E2F targets, G_2M checkpoint, MYC targets (V1 and V2), mTORC1 signaling, inflammatory response, and KRAS signaling up, were strongly activated, whereas the KRAS signaling DN pathway was downregulated, supporting the idea that sotorasib or adagrasib resistance drives cells towards more aggressive, proliferative and *trans*-differentiated states. We then evaluated the most common altered genes and as reported by the Venn diagram in Fig. 2E, 24 genes were upregulated in both sotorasib- and adagrasib-resistant clones (Table S2), whereas 44 and 97 genes were upregulated only in S1-2 and A1-2, respectively. Among the commonly upregulated genes, we focused our attention on the two soluble factors CXCL1 and HGF, which are known to activate the CXCR2 and MET membrane receptors, respectively. The CXCL1/CXCR2 and the HGF/c-MET axes are attractive targets for therapy, with drugs like CXCR2 antagonists (e.g., SB225002) and MET inhibitors showing promise in preclinical and clinical studies [21,41].

3.3. CXCL1/CXCR2 and MET/HGF pathways are activated in sotorasib and adagrasib-resistant clones

The mRNA levels of CXCL1 and HGF were confirmed to be significantly increased in the resistant clones in comparison to the control cells, as demonstrated by RT-PCR analysis (Fig. 3A-B). Furthermore, ELISA assays revealed elevated secretion in the culture medium of the cytokines CXCL1 and HGF in the resistant clones (Fig. 3C-D).

We therefore investigated the signaling pathways that are modulated by HGF and CXCL1. As illustrated in Fig. 3E, a significant increase in phospho-MET was observed in both adagrasib and sotorasib-resistant clones. It is interesting to note that also the MET protein level was increased in cells treated with inhibitors particularly in resistant clones. MET amplification was excluded based on the results of FISH analysis (Fig. S1). Furthermore, resistant clones exhibited increased CXCR2 levels compared to sotorasib or adagrasib H23-treated parental cells, as

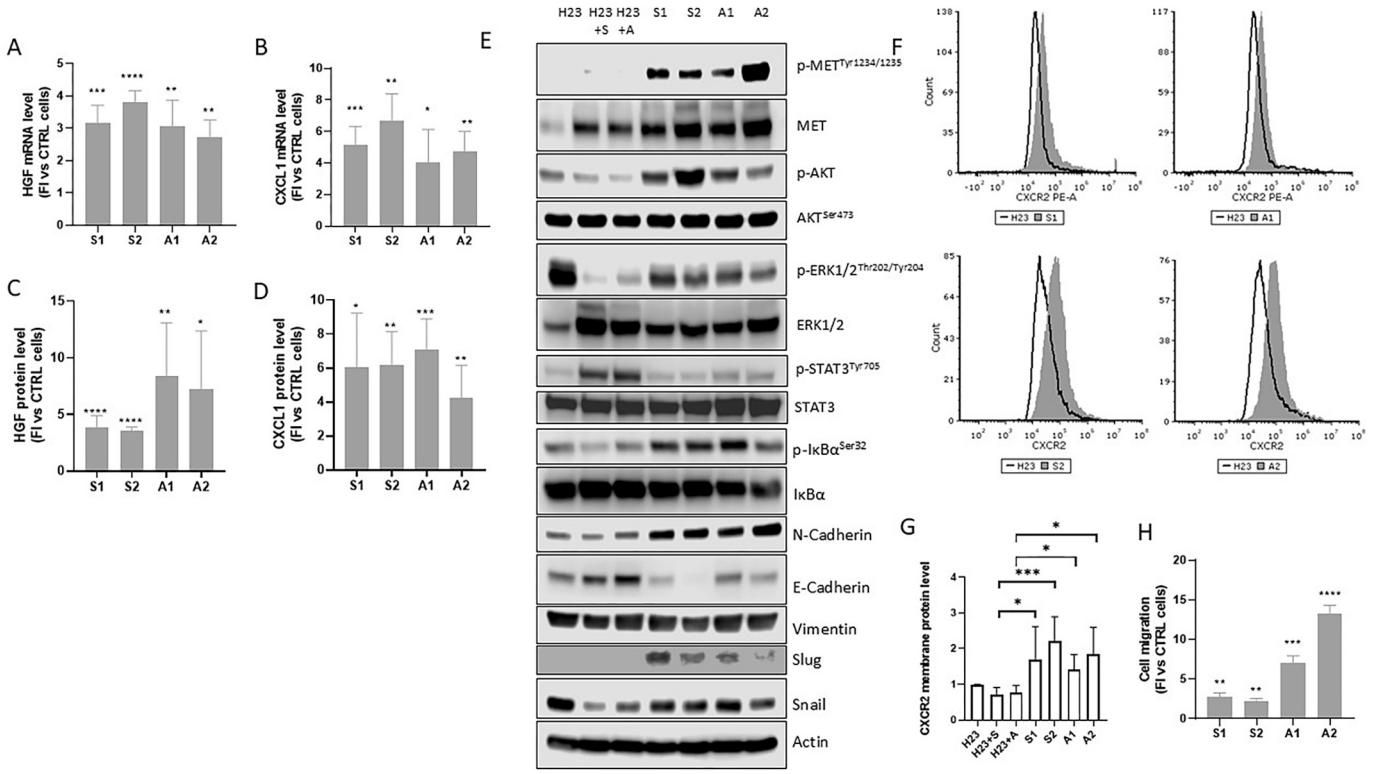

Fig. 3. Evaluation of HGF/c-MET and CXCL1/CXCR2 axes activation in resistant clones. S1, S2, A1 and A2 cells were maintained with 1 and 0.5 μM of sotorasib and adagrasib, respectively and RT-PCR was performed to check the levels of (A) HGF and (B) CXCL1 mRNAs represented as fold increase (FI) vs treated parental cells. Secreted HGF (C) and CXCL1 (D) proteins were evaluated by ELISA assay after 48 h of treatment and represented as fold increase (FI) vs treated parental cells. (E) H23, S1, S2, A1, and A2 cells were treated with 1 or 0.5 μM sotorasib or adagrasib, respectively; protein phosphorylation status of MET, AKT, ERK1/2 STAT3 and IκBα and EMT markers were analyzed by western blotting after 16 h. Flow cytometry representative analysis (F) and quantification (G) of CXCR2 membrane level after 24 h of treatment. (H) Cells were seeded in 8 μm pore transwell and after 16 h cells that have migrated through the membranes were counted under a Phase contrast microscope. Results are expressed as fold change compared to treated parental cells. *$p < 0.05$; **$p < 0.01$; ***$p < 0.001$. A, B, C, D, and G are the average of three independent experiments; E and H are representative of two independent experiments.

evaluated by flow cytometry (Fig. 3F-G).

CXCL1/CXCR2 signaling has been demonstrated to facilitate cell proliferation and survival through PI3K/AKT, MAPK/p38, RAS/ERK and NF-κB pathways [15,23]. Similarly, HGF/c-MET is reported to activate intracellular signaling as PI3K/AKT, FAK, and RAS/ERK axes [42]. Based on these data, ERK1/2 and AKT signaling were analyzed in S1, S2, A1 and A2 cell clones compared to parental cells treated with sotorasib and adagrasib. As reported in Fig. 3E, the immunoblot analysis confirmed the presence of ERK1/2 phosphorylation in our clones as previously reported (Fig. 1E). Moreover, we observed a significant increase in AKT phosphorylation in all the tested clones. This, together with the activation of ERK1/2 signaling, suggests that both pathways are fully engaged in promoting survival and proliferation in these resistant clones. Additionally, the phosphorylation of IκBα increased slightly in resistant clones, indicating that NF-κB may be moving to the nucleus to initiate gene expression and control inflammation, immunity, and cell survival.

Finally, we evaluated the activation of the STAT3 protein, given that the activation of STAT3 signalling may be controlled by the activation of the CXCR2/CXCL1 axis. We demonstrated that the inhibition of KRAS by sotorasib or adagrasib in sensitive cells upregulated STAT3 phosphorylation, however in the resistant clones the level of STAT3 was similar to control cells. These results ruled out the possibility that STAT3 may play a role in sustaining resistance to KRAS inhibitors in our clones.

Both MET and CXCR2 play a crucial role in the EMT by promoting the loss of epithelial characteristics and the gain of mesenchymal traits in cancer cells [43–45]. As reported in Fig. 3E, all the resistant clones exhibited a marked increase in the mesenchymal markers N-cadherin and Slug associated with a decrease in the epithelial marker E-cadherin compared with H23 parental cells. For Snail protein, an increase in its levels was shown in all the clones in comparison with H23 cells treated with both $KRAS^{G12C}$ inhibitors. Resistant cells displayed increased migratory capability as shown in Fig. 3H and failed to generate stable spheroids as parental H23 cells did (Fig. S2); instead, they generated unstable cell aggregates as reported for cancer cells with reduced E-cadherin and high N-cadherin levels [46,47].

These results strongly suggest that the activation of both HGF/c-MET and CXCL1/CXCR2 pathways induced the EMT and promoted migration of all the tested clones.

3.4. The pharmacological inhibition of CXCL1/CXCR2 and HGF/c-MET axes caused a synergistic inhibition of cell proliferation, induced apoptosis and reverted EMT in both sotorasib and adagrasib-resistant clones

Having established that both the HGF-c-MET and the CXCL1-CXCR2 signaling pathways were activated in the resistant clones, we evaluated whether combining specific drugs that target these pathways would produce a synergistic effect in terms of inhibiting cancer cell proliferation. As shown in Fig. 4A-B, we treated the resistant cell clones S2 and A2 with different doses of crizotinib (c-MET inhibitor) and SB225002 (CXCR2/CXCL1 binding inhibitor) in a combined setting to assess the effects of drug interaction. Using the HSA and Bliss model in the Combenefit software, we calculated the additivity, synergism or antagonism produced by the combination of different doses of crizotinib and SB225002. Results shown in Fig. 4 indicated that the combination produced synergistic effects in both clones by using HSA model meanwhile the effects were additive in S2 when Bliss model was used. There was no antagonism in any drug dose combination. These data suggested

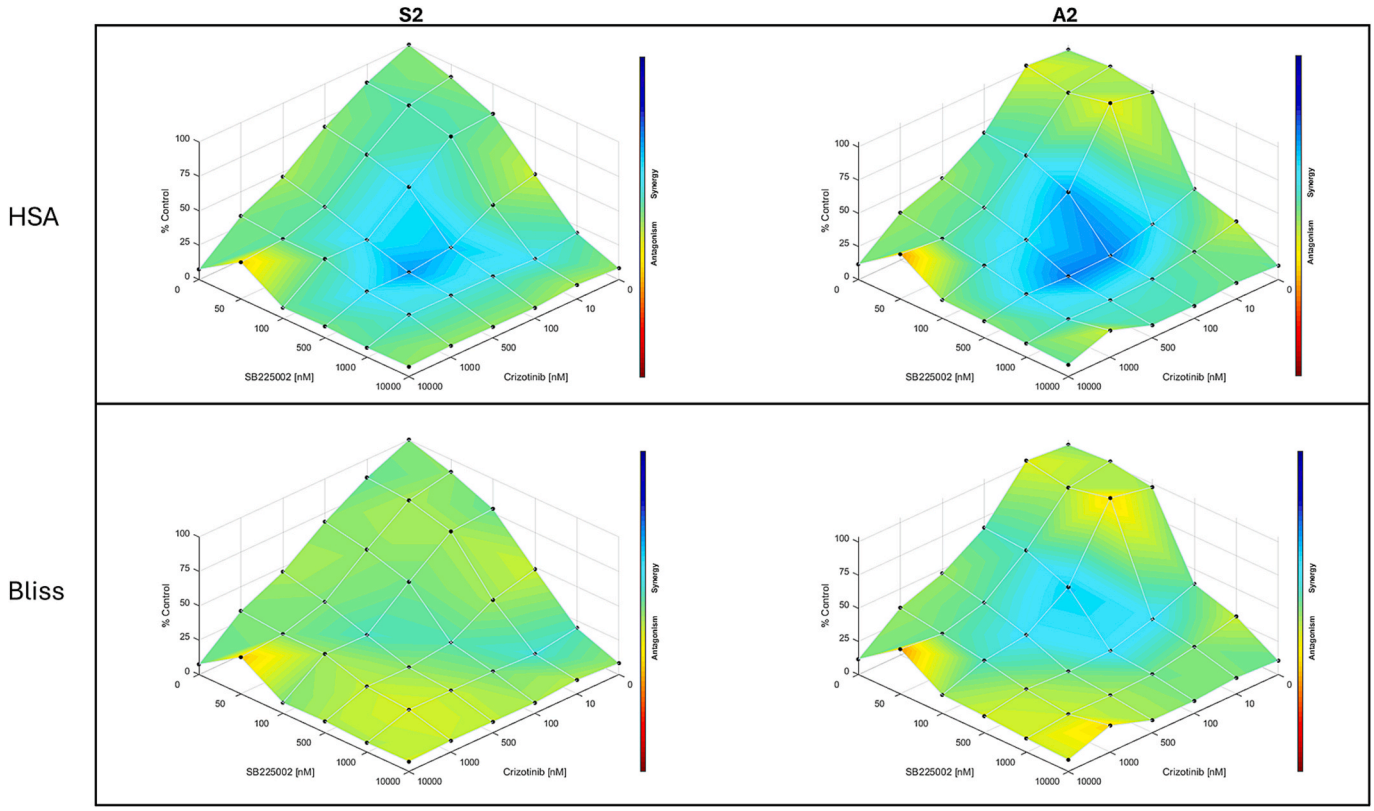

Fig. 4. Isobologram analysis and synergism determination. S2 and A2 cells were treated with increasing doses of crizotinib and SB225002; after 72 h, cell proliferation was assessed by SRB assay, and the effect of this combination was evaluated by Combenefit software (HSA & Bliss Models). Data are representative of three independent experiments.

that dual inhibition of the c-MET and CXCR2 receptors could be a promising strategy for bypassing resistance to KRAS inhibitors.

To further explore this hypothesis, we next evaluated the impact of this combination on the signaling pathways activated in resistant clones. The dose–response of crizotinib and SB225002 in clone A2 (see Fig. S3) indicated that crizotinib inhibited p-MET, p-AKT and p-ERK1/2 at 50 nM and CXCR2 inhibition by SB225002 reduced p-AKT, p-ERK1/2, and p-IκBα at concentrations of 500 nM or higher. The activation of downstream pathways was not fully suppressed, which provides a mechanistic basis for combined therapeutic strategies.

As shown in Fig. 5A, crizotinib–SB225002 combination strongly reduced AKT and ERK1/2 phosphorylation in both the resistant clones. Both single agents but more effectively their combination, promoted a reversal of EMT, as indicated by the reduced expression of the mesenchymal markers' vimentin and N-cadherin and increased expression of the epithelial marker E-cadherin in both S2 and A2 clones Fig. 5B. Moreover, a significant increase in apoptosis, as evaluated by Annexin assay, was observed in the combination treatment compared to either single drug in both clones (Fig. 5C-D).

These results demonstrate that the crizotinib-SB205002 combination reduced cell viability, reversed EMT and induced apoptosis in sotorasib- and adagrasib-resistant clones.

3.5. The combination of SB225002 with crizotinib caused a strong antiproliferative and proapoptotic effect in patient-derived cell cultures

To further explore the rationale behind this combination in the context of primary resistance to $KRAS^{G12C}$ inhibitors, we used two NSCLC cell cultures (ADK-35 and ADK-35a) derived from a PDX established from a patient who experienced rapid progression following third-line sotorasib therapy. As expected, both the cell lines were resistant to sotorasib ($IC_{50} > 5$ μM) (Fig. 6A) and a cross resistance was also demonstrated to adagrasib ($IC_{50} \sim 1$ μM) (Fig. 6B).

To investigate the presence of genetic alterations that could account for the resistance to $KRAS^{G12C}$ inhibitors, a WGS analysis was performed. Both cells retained $KRAS^{G12C}$ mutation, and no secondary KRAS alterations were identified (data not shown). Interestingly, although both cancer cell cultures originated from the same patient, they displayed some distinct genomic alterations (87 and 100 in ADK-35 and ADK 35a, respectively), as indicated in Fig. S4A.

The network map (Fig. S4B) provides a high-resolution perspective on how overlapping (shared) and distinct (clone-specific) gene mutations structurally and functionally drive a spectrum of resistant phenotypes. The study demonstrates how the genetic background of each clone influences the key adaptive pathways. These included DNA repair, cell signaling (e.g. MAPK/PI3K, TGF-β), oxidative stress resistance (e.g. NRF2), and therapy resistance. Indeed, the presence of KEAP1, SKT11, SMARCA4, and TP53 common genetic alterations could account for the resistance to $KRAS^{G12C}$ drugs as previously reported [48,49]. While these alterations may account for the intrinsic resistance to sotorasib and adagrasib, we sought to determine whether targeting the HGF/c-MET and CXCL1/CXCR2 signaling pathways could also prove to be effective in these models.

To this end, we first determined the mRNA and protein levels of HGF and CXCL1 in both ADK-35 and ADK-35a cells. These levels were then compared with those of the S2 clone, which is, as previously described, representative of resistance to sotorasib and is characterized by elevated expression of both the transcript and protein levels of CXCL1 and HGF (see Fig. 3A-B). As illustrated in Fig. 6C-F, mRNA and protein levels for CXCL1 and HGF were higher or at comparable levels than those reported for the S2 clone.

Combining SB225002 and crizotinib produced a robust, synergistic anti-proliferative effect in both ADK-35 and ADK35-a cells as evaluated by the Combenefit software (BLISS and HSA models) (Fig. 7A-B and

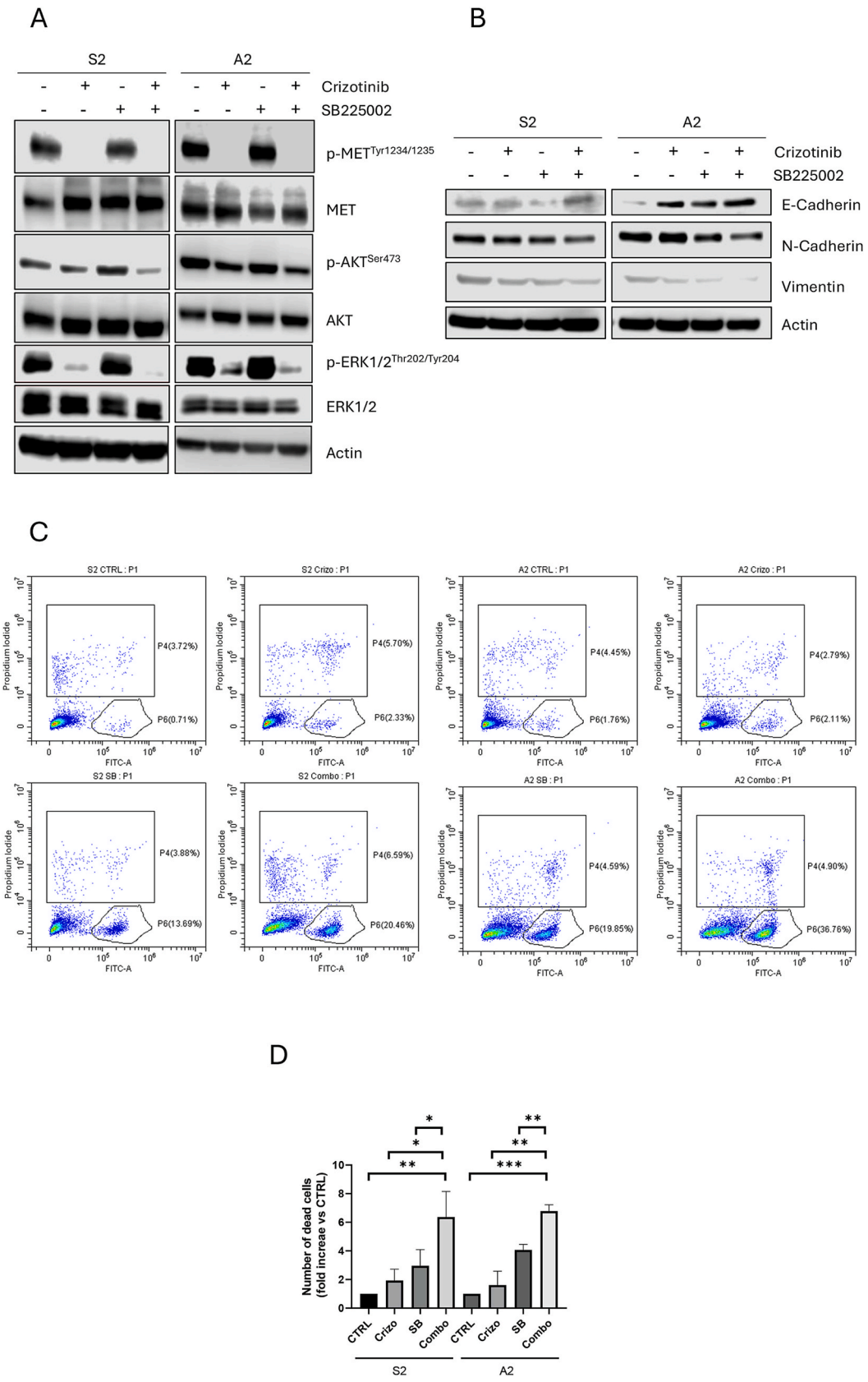

Fig. 5. Effect of the combination of crizotinib and SB225002 on cell proliferation, cell signaling and apoptosis in resistant clones. (A-B) Western blot analyses of indicated proteins in S2 and A2 cells treated with 50 nM crizotinib and 500 nM SB205002 for 1 h (A) and 16 h (B). S2 and A2 cells were treated with crizotinib, SB225002, or the combination for 24 h. Apoptotic cells were detected with the Annexin V staining/flow cytometry (C) and cell death was quantified (D). *p < 0.05; **P < 0.01; ***p < 0.001. A and B are representative of two independent experiments; C is representative of three independent experiments; D is the average of three independent experiments.

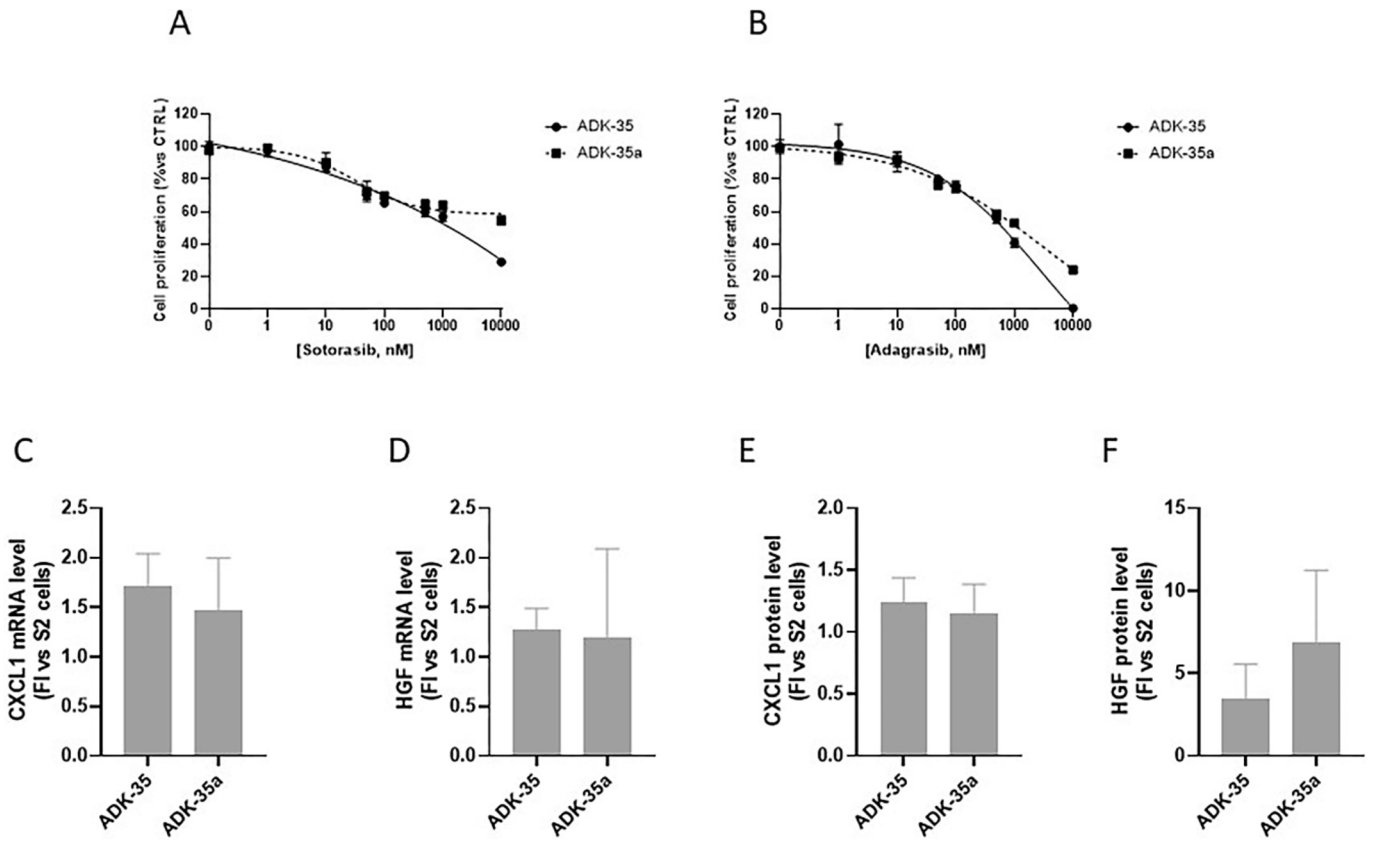

Fig. 6. Evaluation of HGF and CXCL1 mRNAs and protein levels in resistant patient-derived cell cultures. Dose-response of sotorasib (A) and adagrasib (B) in ADK-35 and ADK-35a cells. The levels of CXCL1 (C) and HGF (D) mRNAs were evaluated by RT-PCR and represented as fold increase (FI) vs S2 cells. Secreted CXCL1 (E) and HGF (F) proteins were evaluated by ELISA assay and represented as fold increase (FI) vs S2 cells. A and B are representative of three independent experiments; C-F are the average of three independent experiments.

Fig. S5) and by holographic image analysis (Fig. 7C-D) with the inhibition of AKT and ERK1/2 phosphorylation (Fig. 7E-F) providing further evidence to support our therapeutic approach. This marked antiproliferative effect was also associated with an increase in apoptosis already detectable after 24 h (Fig. 7G-H), when the cells were exposed to the crizotinib–SB205002 combination.

4. Discussion

Resistance to KRAS inhibitors such as sotorasib and adagrasib remains a major therapeutic challenge in NSCLC. In this study, we demonstrate for the first time that resistance to $KRAS^{G12C}$ inhibition is linked to elevated expression and secretion of CXCL1 and HGF, leading to activation of their respective receptors, CXCR2 and c-MET, through an autocrine mechanism. Notably, this phenotype was consistently observed across all resistant clones, whether displaying acquired or intrinsic resistance and independent of underlying genetic alterations, highlighting a common behavior associated with KRAS inhibition resistance. Remarkably, simultaneous blockade of the HGF/c-MET and CXCL1/CXCR2 axes produced a synergistic effect, suppressing tumor cell proliferation and inducing apoptosis, thereby providing a compelling rationale for dual targeting as a therapeutic strategy to overcome KRAS inhibitors resistance.

CXCL1 is significantly upregulated in lung adenocarcinoma tissues and correlates with advanced stage and poor overall survival [50]. Enhanced activation of the CXCL1/CXCR2 axis contributes to drug resistance by promoting cancer cell survival, migration, and immune evasion. The underlying mechanisms include NF-κB activation, upregulation of BCL-2, induction of autophagy, reduced expression of superoxide dismutase 1 (SOD1), recruitment of myeloid-derived suppressor cells (MDSCs) and neutrophils, and increased expression of PD-L1 [21]. Interestingly, in some cases, the increase in the expression of CXCL1 and other CXCR2 ligands may not be a direct mechanism but a marker of chemoresistance [51].

Abnormal activation of HGF/c-MET signaling and its downstream pathway are present in a variety of tumors, and they are associated with poor prognosis and drug resistance. Overexpression or constitutive activation of c-MET, and secretion of HGF leading to an autocrine activation loop are reported as mechanisms of c-MET-driven chemoresistance [52].

MET amplification has been reported as a mechanism of sotorasib resistance in H23 NSCLC cells-derived clones [31] and its clinical relevance has been very recently reported by Riedel et al [53]. A retrospective analysis indicated that in 4 out of 9 patients progressed to sotorasib a high-level MET amplification was detected by FISH, and one patient achieved a partial response to the combination of sotorasib and of the MET inhibitor tepotinib. Preclinical data with tepotinib plus the V ATPase inhibitor omeprazole demonstrated robust synergistic activity in KRAS mutant models, including sotorasib resistant cells, thereby validating MET directed combinations as an effective strategy to revert $KRAS^{G12C}$ inhibitor resistance [54].

In the resistant models under our investigation, a significant increase in phospho-MET was observed in both adagrasib-resistant and sotorasib-resistant clones. Furthermore, an increase in MET protein level was also noted. However, the results of FISH analysis excluded the presence of MET amplification. Moreover, RNAseq analysis did not show increased transcription of the c-MET gene. Our data indicated a high level of c-MET in the resistant clones without gene amplification, and this observation has been previously reported in some ALK-positive or EGFR-mutated NSCLC patients [55]. Other mechanisms, such as increased

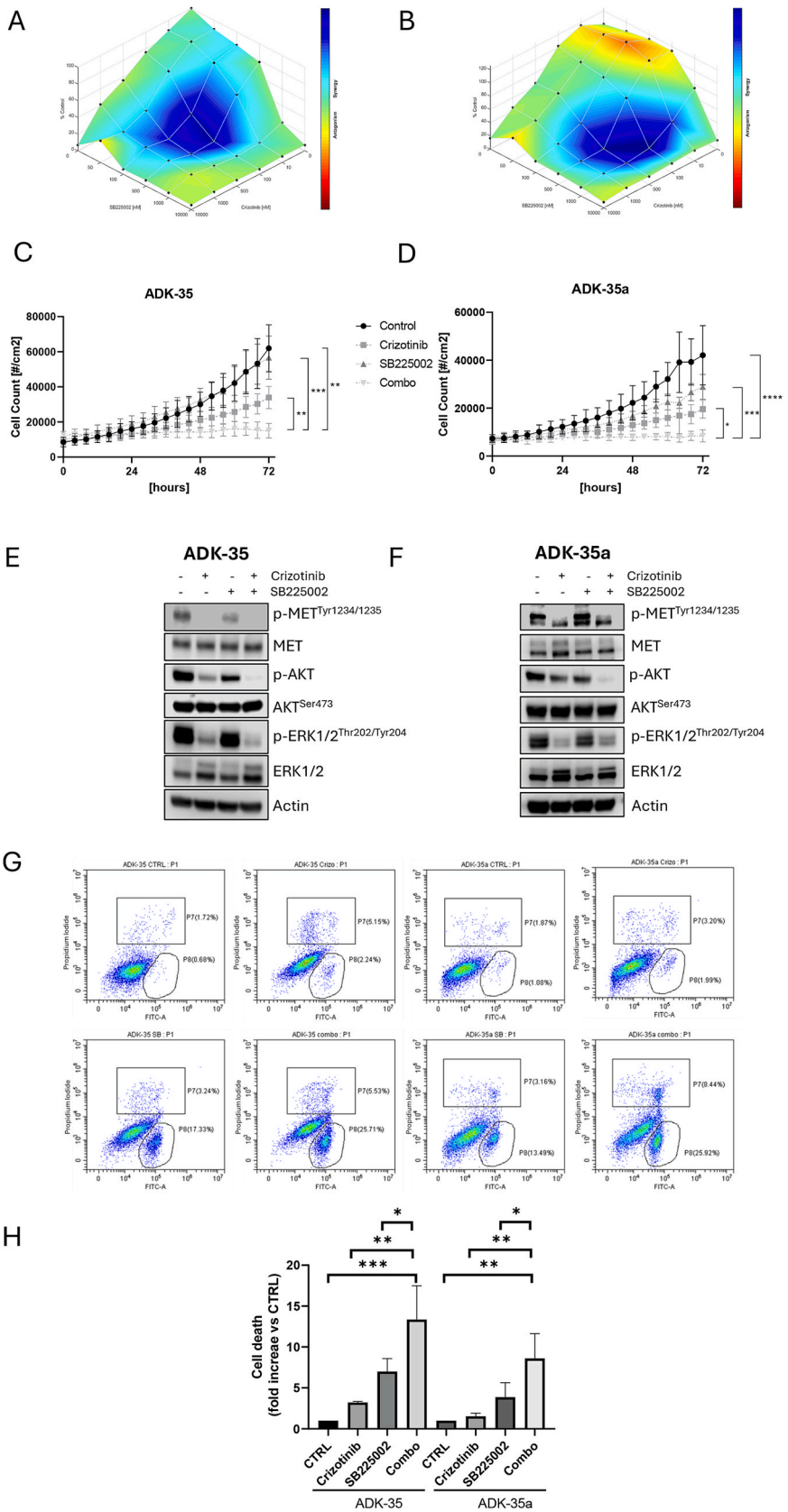

(caption on next page)

Fig. 7. Effects of the combination of crizotinib and SB225002 in resistant patient-derived cell cultures. ADK-35 (A) and ADK-35a (B) cells were treated with increasing doses of crizotinib and SB225002 and after 72 h, cell proliferation was assessed by SRB assay, and the effect of this combination was evaluated by Combenefit software (Bliss model) and by holographic image analysis (C-D). Western blot analysis of indicated proteins in ADK-35 (E) and ADK-35a (F) cells treated with 50 nM crizotinib, 500 nM SB225002 or their combination for 1 h. (G-H) ADK-35 and ADK-35a cells were treated with 50 nM crizotinib, 500 nM SB205002, or their combination for 24 h and apoptotic cells were detected with the Annexin V staining and quantified. *$p < 0.05$; **$P < 0.01$; ***$p < 0.001$; ****$p < 0.0001$. A-F are representative of two independent experiments; G is representative of three independent experiments; H is the average of three independent experiments.

translation of the c-MET protein or c-MET protein stabilization, could be responsible for c-MET overexpression [56].

MET-amplified H23ARC11 cells [31] expressed higher levels of phosphorylated AKT than H23 cells and MET knockdown diminished the AKT activation recovering sotorasib sensitivity in H23ARC11 cells. Adachi et al. [57] reported that sotorasib-resistant NSCLC cell lines exhibited IGFR-IRS1 pathway activation able to sustain PI3K phosphorylation in the presence of sotorasib. The use of a PI3K inhibitor restored sensitivity to sotorasib. AKT phosphorylation was increased in all our resistant clones suggesting that this pathway was involved in promoting survival and proliferation in the presence of KRAS inhibitors. Crizotinib alone failed to suppress AKT phosphorylation that was instead almost completely inhibited when crizotinib was combined with the CXCR2 inhibitor SB225002. These data suggest that both MET and CXCR2 axes promoted AKT activation and that the suppression of either these two pathways was important to achieve a suppression of proliferation and viability of resistant cells.

We also demonstrated that $KRAS^{G12C}$ inhibition in H23 parental cells resulted in increased STAT3 phosphorylation. In the resistant clones, however, the level of STAT3 was similar to that in control cells. These results confirmed the inverse relationship between STAT3 and ERK phosphorylation reported in previous papers. Pan and coauthors [58] have recently demonstrated that the ERK inhibitor selumetinib induced STAT3 activation and that the STAT3 inhibitor napabucasin led to ERK activation in KRAS mutated NSCLC cells and MEK inhibitors efficiently blocked the phosphorylation of ERK1/2 while STAT3 signaling was rapidly activated in esophageal squamous cell carcinoma [59].

In H23 cells, sotorasib and adagrasib inhibited ERK1/2 phosphorylation, resulting in increased STAT3 activation. By contrast, RAS inhibitors failed to inhibit ERK1/2 activation in resistant clones, consequently reducing STAT3 phosphorylation to basal levels. These results ruled out the possibility that STAT3 plays a role in sustaining resistance to sotorasib in our clones.

Genomic analysis performed in sotorasib, and adagrasib-resistant H23-derived clones did not clarify the mechanism by which resistant cells produce and secrete CXCL1 and HGF. In these clones, we did not observe a common genetic alteration responsible for resistance. The 7 missense variants were jointly analyzed with the four biologically relevant genes differently expressed in sotorasib and adagrasib-resistant clones, CXCL1, HGF and their receptors CXCR2 and MET. The resulting network comprised 11 nodes connected by 11 edges with a PPI enrichment p-value $p = 8.3x10^{-5}$. The network showed the CSF3R gene as pivotal between genes harboring missense variants and biologically relevant genes. Of note, significant KEGG pathways were observed, such as “Pathways in cancer” (FDR = 0.0227; involving MSH6, CSF3R, HGF, and MET genes), “Cytokine-cytokine receptor interaction” (FDR = 0.0380; involving CSF3R, CXCL1, and CXCR2 genes), and “PI3K-AKT signaling pathway (FDR = 0.0412; involving CSF3R, HGF, and MET genes). However, CSF3R was a variant detected only in S1 clone with a frequency of 12 %.

WGS analysis performed in ADK cell cultures derived from sotorasib-resistant patient-derived xenografts showed the presence of STK11, SMARCA4, and TP53 as common genetic alterations that could be responsible for the resistance to $KRAS^{G12C}$ inhibitors, as previously reported [49]. Loss and/or somatic mutation of STK11 in tumor cells has been reported to lead to the upregulation of several cytokines including CXCL1 [60] and mutant p53 drives CXCL1 expression in pancreatic [61] and breast cancer [62]. However, a direct correlation in our cell lines remains to be fully clarified.

Sensitivity to the $KRAS^{G12C}$ inhibitor sotorasib has been linked to an epithelial-like phenotype, while the induction of EMT has been associated with acquired resistance to this drug [57]. The role of c-MET in driving EMT is well known [45,63]; notably, the CXCR2 receptor has also been implicated in promoting EMT across various cancer types. The CXCR2/CXCL5 axis induces EMT in hepatocellular carcinoma cells by activating the PI3K/AKT/GSK-3β/Snail signaling pathway [64]. In renal cell carcinoma CXCR2 and Snail-1 induce EMT, enhancing tumor invasiveness and metastatic potential via the ERK1/2 signaling pathway [65]. Our data confirms that the activation of the HGF/c-MET and CXCL1/CXCR2 axes is associated with cadherin switching, which is characterized by an increase in N-cadherin, Snail and Slug, and a decrease in E-cadherin.

The therapeutic potential of targeting CXCL1 and its receptor, CXCR2, in cancer treatment has been recently reviewed by Korbecki and collaborators [21]. SB225002, a well-known CXCR2 antagonist, has demonstrated antitumor properties against a variety of cancers [21]. SB225002 was confirmed to inhibit the proliferation of lung cancer cells, induce cell apoptosis, promote lung cancer cell senescence, and inhibit EMT. In murine models of lung cancer, SB225002 has been shown to inhibit lung tumour growth by decreasing immune-suppressing neutrophil infiltration, augmenting the activation of CD8 + T cells, and improving the therapeutic effect of cisplatin by modulating the tumour microenvironment [18].

Crizotinib is a multitarget inhibitor, its main targets being ALK, ROS1, and MET. Crizotinib has shown promise in overcoming acquired resistance sustained by activation of the HGF/c-MET axis in various cancers [41]. The association between SB225002 and crizotinib results in a significant reduction in cell proliferation and induction of apoptosis in both sotorasib and adagrasib-resistant cells (both with acquired and primary resistance). These effects appear to be the result of inhibition of AKT and ERK1/2 phosphorylation associated with EMT reversal. It is well known that AKT signaling is a key driver of EMT by regulating transcription factors that suppress epithelial traits and promote mesenchymal features, cooperating with other pathways to enhance tumor cell invasion and metastasis: it has been reported that pharmacological EMT reversion is a strategy to fight cancer cells with acquired resistance to $KRAS^{G12C}$ inhibitors [57].

In our context, a full inhibition of signaling and EMT is obtained with the simultaneous addiction of both the drugs, suggesting that both axes contributed to bypass the antiproliferative effect of $KRAS^{G12C}$ inhibitors. Although the causality within HGF/c-MET and CXCL1/CXCR2 axes was supported pharmacologically, complementary genetic gain- and loss-of-function studies will further strengthen mechanistic inference. The findings of this study should be considered in light of the following limitations: in vitro models do not capture the complexity of the tumour microenvironment, so co-colture models of macrophages and lung cancer cells and in vivo validation of the combination in xenograft models are warranted for defining also the optimal dosage and sequencing of combination therapy. NF-κB and CXCR2 are tightly linked in inflammatory and tumor biology through reciprocal regulation of chemokine signaling. Their crosstalk creates a loop that sustains leukocyte recruitment, angiogenesis, and survival signals. Western blot analysis (see new Fig. 3E) indicates that IκBα phosphorylation is increased in resistant clones, suggesting that NF-κB moves to the nucleus to initiate gene expression and control inflammation and immunity. Investigating the role of the CXCL1/CXCR2 receptor and NF-κB in

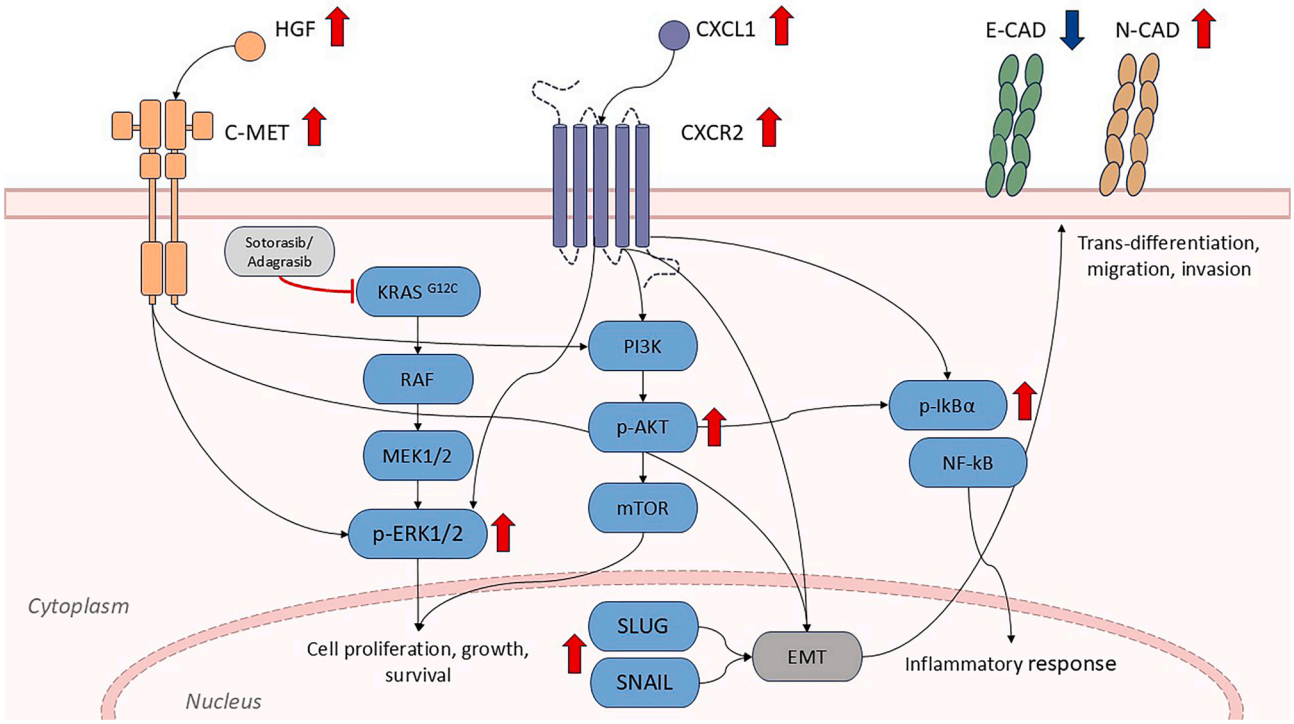

Fig. 8. Graphical abstract. CXCR2 and c-MET signaling networks sustain resistance to KAS^{G12C} inhibitors.

recruiting immune cells and inducing inflammation is of great interest. However, this issue falls outside the scope of the present manuscript and requires further dedicated research.

In summary, as depicted in Fig. 8, CXCR2 and c-MET engage overlapping and reinforcing signaling networks that contribute to the maintenance of resistance to KAS^{G12C} inhibitors. This correlation is manifested through shared downstream effectors (PI3K/AKT, MAPK), and EMT promotion. To our knowledge, no previous studies have investigated the combination of a CXCR2 inhibitor with a c-MET inhibitor in the context of resistance to KRAS-targeted therapies. From a clinical perspective, the co-targeting approach employed in the present study offers a novel perspective on a potentially effective strategy for bypassing resistance, particularly in tumors exhibiting mesenchymal features and an inflammatory tumor microenvironment.

CRediT authorship contribution statement

A. Cavazzoni: Writing – review & editing, Writing – original draft, Investigation, Conceptualization. **M. Pagano Mariano:** Validation, Investigation, Conceptualization. **A. Palladini:** Methodology, Investigation. **G. Digiacomo:** Investigation, Data curation, Conceptualization. **S. La Monica:** Investigation, Data curation, Conceptualization. **M. Bonelli:** Investigation, Data curation. **M. Galetti:** Investigation, Data curation. **I. Pace:** Methodology, Investigation. **R. Roncarati:** Writing – review & editing, Methodology, Investigation. **E. Giovannetti:** Writing – review & editing, Methodology, Investigation. **P. Aretini:** Writing – review & editing, Methodology. **R. Minari:** Methodology, Investigation. **M. Treccani:** Formal analysis. **M. Pluchino:** Methodology, Investigation. **C.A. Lagrasta:** Methodology. **S. Angelicola:** Methodology, Investigation. **G. Mazzaschi:** Writing – review & editing. **P. Bordi:** Writing – review & editing. **F. Gelsomino:** Writing – review & editing, Supervision. **F. Agustoni:** Supervision. **P.G. Petronini:** Writing – review & editing, Supervision. **M. Tiseo:** Writing – review & editing, Supervision. **M. Ferracin:** Writing – review & editing, Supervision, Methodology, Investigation. **R. Alfieri:** Writing – review & editing, Writing – original draft, Supervision, Funding acquisition, Conceptualization.

Funding

This research has financially been supported by the Program "FIL-Quota Incentivante" of University of Parma and co-sponsored by Fondazione Cariparma (PI RA). The work was also supported by Associazione Augusto per la Vita, Novellara, RE, Italy and by AVOPRORIT, Parma, Italy.

The founders had no role in study design, data collection and analysis, decision to publish, or preparation of the manuscript.

Declaration of competing interest

The authors declare that they have no financial conflicts of interest or personal affiliations that may be perceived as potentially influencing the findings presented in this manuscript. M.Tiseo received speakers' and consultants' fee from Astra-Zeneca, Pfizer, Eli-Lilly, BMS, Novartis, Roche, MSD, Boehringer Ingelheim, Takeda, Amgen, Merck, Sanofi, Johnson & Johnson, Pierre Fabre, Regeneron, BeiOne, Daiichi Sankyo and Accord. He received institutional research grants from Astra-Zeneca, Boehringer Ingelheim, Sanofi and Roche. He received travel support from Amgen, Pierre Fabre, Pfizer, Takeda and Roche. F.Gelsomino. has had a consulting or advisory role with Novartis, Eli Lilly, Pfizer, Bristol Myers Squibb, AstraZeneca, and Regeneron.

Acknowledgments

The PDX cultures were provided by F. Gelsomino as part of a study supported by Ricerca Finalizzata Ministero della Salute 2018 Grant, number GR-2018-12368031 (PI F. Gelsomino)

Appendix A. Supplementary data

Supplementary data to this article can be found online at https://doi.org/10.1016/j.lungcan.2026.108939.

References

[1] L.E. Hendriks, K.M. Kerr, J. Menis, T.S. Mok, U. Nestle, A. Passaro, S. Peters, D. Planchard, E.F. Smit, B.J. Solomon, G. Veronesi, M. Reck, E.G.C.E.a. clinicalguidelines@esmo.org, Oncogene-addicted metastatic non-small-cell lung cancer: ESMO Clinical Practice Guideline for diagnosis, treatment and follow-up, Ann. Oncol. 34 (4) (2023) 339–357.

[2] L.E. Hendriks, K.M. Kerr, J. Menis, T.S. Mok, U. Nestle, A. Passaro, S. Peters, D. Planchard, E.F. Smit, B.J. Solomon, G. Veronesi, M. Reck, E.G.C.E.a. clinicalguidelines@esmo.org, Non-oncogene-addicted metastatic non-small-cell lung cancer: ESMO Clinical Practice Guideline for diagnosis, treatment and follow-up, Ann. Oncol. 34 (4) (2023) 358–376.

[3] R.B. Scharpf, A. Balan, B. Ricciuti, J. Fiksel, C. Cherry, C. Wang, M.L. Lenoue-Newton, H.A. Rizvi, J.R. White, A.S. Baras, J. Anaya, B.V. Landon, M. Majcherska-Agrawal, P. Ghanem, J. Lee, L. Raskin, A.S. Park, H. Tu, H. Hsu, K.C. Arbour, M. M. Awad, G.J. Riely, C.M. Lovly, V. Anagnostou, Genomic Landscapes and Hallmarks of Mutant RAS in Human Cancers, Cancer Res. 82 (21) (2022) 4058–4078.

[4] C. Johnson, D.L. Burkhart, K.M. Haigis, Classification of KRAS-Activating Mutations and the Implications for Therapeutic intervention, Cancer Discov. 12 (4) (2022) 913–923.

[5] T.F. Burns, H. Borghaei, S.S. Ramalingam, T.S. Mok, S. Peters, Targeting KRAS-Mutant Non-Small-Cell Lung Cancer: one Mutation at a Time, with a Focus on KRAS G12C Mutations, J. Clin. Oncol. 38 (35) (2020) 4208–4218.

[6] H.A. Blair, Sotorasib: first Approval, Drugs 81 (13) (2021) 1573–1579.

[7] S. Dhillon, Adagrasib: first Approval, Drugs 83 (3) (2023) 275–285.

[8] E.C. Nakajima, N. Drezner, X. Li, P.S. Mishra-Kalyani, Y. Liu, H. Zhao, Y. Bi, J. Liu, A. Rahman, E. Wearne, I. Ojofeitimi, L.T. Hotaki, D. Spillman, R. Pazdur, J. A. Beaver, H. Singh, FDA Approval Summary: Sotorasib for KRAS G12C-mutated Metastatic NSCLC, Clin. Cancer Res. 28 (8) (2022) 1482–1486.

[9] F. Barlesi, W. Yao, M. Duruisseaux, L. Doucet, A.A. Martinez, V. Gregorc, O. Juan-Vidal, S. Lu, C. De Bondt, F. de Marinis, H. Linardou, Y.C. Kim, R. Jotte, E. Felip, G. Lo Russo, M. Reck, M.F. Michenzie, W. Yang, J.N. Meade, B. Korytowsky, T.S. K. Mok, K. Investigators, Adagrasib versus docetaxel in KRAS(G12C)-mutated non-small-cell lung cancer (KRYSTAL-12): a randomised, open-label, phase 3 trial, Lancet 406 (10503) (2025) 615–626.

[10] M. Sattler, A. Mohanty, P. Kulkarni, R. Salgia, Precision oncology provides opportunities for targeting KRAS-inhibitor resistance, Trends Cancer 9 (1) (2023) 42–54.

[11] Y. Zhao, Y.R. Murciano-Goroff, J.Y. Xue, A. Ang, J. Lucas, T.T. Mai, A.F. Da Cruz Paula, A.Y. Saiki, D. Mohn, P. Achanta, A.E. Sisk, K.S. Arora, R.S. Roy, D. Kim, C. Li, L.P. Lim, M. Li, A. Bahr, B.R. Loomis, E. de Stanchina, J.S. Reis-Filho, B. Weigelt, M. Berger, G. Riely, K.C. Arbour, J.R. Lipford, B.T. Li, P. Lito, Diverse alterations associated with resistance to KRAS(G12C) inhibition, Nature 599 (7886) (2021) 679–683.

[12] N. Tanaka, J.J. Lin, C. Li, M.B. Ryan, J. Zhang, L.A. Kiedrowski, A.G. Michel, M. U. Syed, K.A. Fella, M. Sakhi, I. Baiev, D. Juric, J.F. Gainor, S.J. Klempner, J. K. Lennerz, G. Siravegna, L. Bar-Peled, A.N. Hata, R.S. Heist, R.B. Corcoran, Clinical acquired Resistance to KRAS(G12C) Inhibition through a Novel KRAS Switch-II Pocket Mutation and Polyclonal Alterations Converging on RAS-MAPK Reactivation, Cancer Discov. 11 (8) (2021) 1913–1922.

[13] M.T. Chow, A.D. Luster, Chemokines in cancer, Cancer Immunol. Res. 2 (12) (2014) 1125–1131.

[14] M. Yi, T. Li, M. Niu, H. Zhang, Y. Wu, K. Wu, Z. Dai, Targeting cytokine and chemokine signaling pathways for cancer therapy, Signal Transduct. Target. Ther. 9 (1) (2024) 176.

[15] S. Raza, S. Rajak, A. Tewari, P. Gupta, N. Chattopadhyay, R.A. Sinha, B. Chakravarti, Multifaceted role of chemokines in solid tumors: from biology to therapy, Semin. Cancer Biol. 86 (Pt 3) (2022) 1105–1121.

[16] I. Kogan-Sakin, M. Cohen, N. Paland, S. Madar, H. Solomon, A. Molchadsky, R. Brosh, Y. Buganim, N. Goldfinger, H. Klocker, J.A. Schalken, V. Rotter, Prostate stromal cells produce CXCL-1, CXCL-2, CXCL-3 and IL-8 in response to epithelia-secreted IL-1, Carcinogenesis 30 (4) (2009) 698–705.

[17] P. Saintigny, E. Massarelli, S. Lin, Y.H. Ahn, Y. Chen, S. Goswami, B. Erez, M. S. O'Reilly, D. Liu, J.J. Lee, L. Zhang, Y. Ping, C. Behrens, L.M. Solis Soto, J. V. Heymach, E.S. Kim, R.S. Herbst, S.M. Lippman, W.K. Wistuba II, J.M. Hong, J.S. K. Kurie, CXCR2 expression in tumor cells is a poor prognostic factor and promotes invasion and metastasis in lung adenocarcinoma, Cancer Res. 73 (2) (2013) 571–582.

[18] Y. Cheng, F. Mo, Q. Li, X. Han, H. Shi, S. Chen, Y. Wei, X. Wei, Targeting CXCR2 inhibits the progression of lung cancer and promotes therapeutic effect of cisplatin, Mol. Cancer 20 (1) (2021) 62.

[19] A. Spaks, Role of CXC group chemokines in lung cancer development and progression, J. Thorac. Dis. 9 (Suppl 3) (2017) S164–S171.

[20] C. Yang, H. Yu, R. Chen, K. Tao, L. Jian, M. Peng, X. Li, M. Liu, S. Liu, CXCL1 stimulates migration and invasion in ER-negative breast cancer cells via activation of the ERK/MMP2/9 signaling axis, Int. J. Oncol. 55 (3) (2019) 684–696.

[21] J. Korbecki, M. Bosiacki, M. Pilarczyk, M. Kot, P. Defort, I. Walaszek, D. Chlubek, I. Baranowska-Bosiacka, The CXCL1-CXCR2 Axis as a Component of Therapy Resistance, a source of Side Effects in Cancer Treatment, and a Therapeutic Target, Cancers (Basel) 17 (10) (2025).

[22] Y.L. Park, H.P. Kim, C.Y. Ock, D.W. Min, J.K. Kang, Y.J. Lim, S.H. Song, S.W. Han, T.Y. Kim, EMT-mediated regulation of CXCL1/5 for resistance to anti-EGFR therapy in colorectal cancer, Oncogene 41 (14) (2022) 2026–2038.

[23] J. Fu, X. Su, Z. Li, L. Deng, X. Liu, X. Feng, J. Peng, HGF/c-MET pathway in cancer: from molecular characterization to clinical evidence, Oncogene 40 (28) (2021) 4625–4651.

[24] M.S. Tsao, L. Sholl, M. Shiller, P. Illei, M.B. Wistuba II, K.A. Beasley, A. Schalper, P. Simmons, S. Ansell, M.-K. Beruti, MET (c-Met) protein overexpression is an emerging protein biomarker in non-small cell lung cancer, NPJ Precis, Oncol 9 (1) (2025) 369.

[25] P.C. Ma, R. Jagadeeswaran, S. Jagadeesh, M.S. Tretiakova, V. Nallasura, E.A. Fox, M. Hansen, E. Schaefer, K. Naoki, A. Lader, W. Richards, D. Sugarbaker, A. N. Husain, J.G. Christensen, R. Salgia, Functional expression and mutations of c-Met and its therapeutic inhibition with SU11274 and small interfering RNA in non-small cell lung cancer, Cancer Res. 65 (4) (2005) 1479–1488.

[26] B. Ko, T. He, S. Gadgeel, B. Halmos, MET/HGF pathway activation as a paradigm of resistance to targeted therapies, Ann Transl Med 5 (1) (2017) 4.

[27] G. Minuti, F. Cappuzzo, R. Duchnowska, J. Jassem, A. Fabi, T. O'Brien, A. D. Mendoza, L. Landi, W. Biernat, B. Czartoryska-Arlukowicz, T. Jankowski, D. Zuziak, J. Zok, B. Szostakiewicz, M. Foszczynska-Kloda, A. Tempinska-Szalach, E. Rossi, M. Varella-Garcia, Increased MET and HGF gene copy numbers are associated with trastuzumab failure in HER2-positive metastatic breast cancer, Br. J. Cancer 107 (5) (2012) 793–799.

[28] Y. Qin, J. Roszik, C. Chattopadhyay, Y. Hashimoto, C. Liu, Z.A. Cooper, J.A. Wargo, P. Hwu, S. Ekmekcioglu, E.A. Grimm, Hypoxia-Driven Mechanism of Vemurafenib Resistance in Melanoma, Mol. Cancer Ther. 15 (10) (2016) 2442–2454.

[29] E.Y. Rosen, M.L. Johnson, S.E. Clifford, R. Somwar, J.F. Kherani, J. Son, A. A. Bertram, M.A. Davare, E. Gladstone, E.V. Ivanova, D.N. Henry, E.M. Kelley, M. Lin, M.S.D. Milan, B.C. Nair, E.A. Olek, J.E. Scanlon, M. Vojnic, K. Ebata, J. F. Hechtman, B.T. Li, L.M. Sholl, B.S. Taylor, M. Ladanyi, P.A. Janne, S. M. Rothenberg, A. Drilon, G.R. Oxnard, Overcoming MET-Dependent Resistance to Selective RET Inhibition in patients with RET Fusion-positive Lung Cancer by Combining Selpercatinib with Crizotinib, Clin. Cancer Res. 27 (1) (2021) 34–42.

[30] K. Qin, L. Hong, J. Zhang, X. Le, MET Amplification as a Resistance driver to TKI Therapies in Lung Cancer: Clinical challenges and Opportunities, Cancers (Basel) 15 (3) (2023).

[31] S. Suzuki, K. Yonesaka, T. Teramura, T. Takehara, R. Kato, H. Sakai, K. Haratani, J. Tanizaki, H. Kawakami, H. Hayashi, K. Sakai, K. Nishio, K. Nakagawa, KRAS Inhibitor Resistance in MET-Amplified KRAS (G12C) Non-Small Cell Lung Cancer Induced by RAS- and Non-RAS-Mediated Cell Signaling Mechanisms, Clin. Cancer Res. 27 (20) (2021) 5697–5707.

[32] T. Nomura, N. Tamaoki, A. Takakura, H. Suemizu, Basic concept of development and practical application of animal models for human diseases, Curr. Top. Microbiol. Immunol. 324 (2008) 1–24.

[33] H. Li, R. Durbin, Fast and accurate short read alignment with Burrows-Wheeler transform, Bioinformatics 25 (14) (2009) 1754–1760.

[34] P. Danecek, J.K. Bonfield, J. Liddle, J. Marshall, V. Ohan, M.O. Pollard, A. Whitwham, T. Keane, S.A. McCarthy, R.M. Davies, H. Li, Twelve years of SAMtools and BCFtools, GigaScience 10 (2) (2021).

[35] P. Danecek, A. Auton, G. Abecasis, C.A. Albers, E. Banks, M.A. DePristo, R. E. Handsaker, G. Lunter, G.T. Marth, S.T. Sherry, G. McVean, R. Durbin, G., Genomes Project Analysis, the variant call format and VCFtools, Bioinformatics 27 (15) (2011) 2156–2158.

[36] D. Szklarczyk, K. Nastou, M. Koutrouli, R. Kirsch, F. Mehryary, R. Hachilif, D. Hu, M.E. Peluso, Q. Huang, T. Fang, N.T. Doncheva, S. Pyysalo, P. Bork, L.J. Jensen, C. von Mering, The STRING database in 2025: protein networks with directionality of regulation, Nucleic Acids Res. 53 (D1) (2025) D730–D737.

[37] M. Ashburner, C.A. Ball, J.A. Blake, D. Botstein, H. Butler, J.M. Cherry, A.P. Davis, K. Dolinski, S.S. Dwight, J.T. Eppig, M.A. Harris, D.P. Hill, L. Issel-Tarver, A. Kasarskis, S. Lewis, J.C. Matese, J.E. Richardson, M. Ringwald, G.M. Rubin, G. Sherlock, Gene ontology: tool for the unification of biology, The Gene Ontology Consortium, Nat Genet 25 (1) (2000) 25–29.

[38] C. Gene Ontology, S.A. Aleksander, J. Balhoff, S. Carbon, J.M. Cherry, H. J. Drabkin, D. Ebert, M. Feuermann, P. Gaudet, N.L. Harris, D.P. Hill, R. Lee, H. Mi, S. Moxon, C.J. Mungall, A. Muruganugan, T. Mushayahama, P.W. Sternberg, P. D. Thomas, K. Van Auken, J. Ramsey, D.A. Siegele, R.L. Chisholm, P. Fey, M. C. Aspromonte, M.V. Nugnes, F. Quaglia, S. Tosatto, M. Giglio, S. Nadendla, G. Antonazzo, H. Attrill, G. Dos Santos, S. Marygold, V. Strelets, C.J. Tabone, J. Thurmond, P. Zhou, S.H. Ahmed, P. Asanitthong, D. Luna Buitrago, M.N. Erdol, M.C. Gage, M. Ali Kadhum, K.Y.C. Li, M. Long, A. Michalak, A. Pesala, A. Pritazahra, S.C.C. Saverimuttu, R. Su, K.E. Thurlow, R.C. Lovering, C. Logie, S. Oliferenko, J. Blake, K. Christie, L. Corbani, M.E. Dolan, H.J. Drabkin, D.P. Hill, L. Ni, D. Sitnikov, C. Smith, A. Cuzick, J. Seager, L. Cooper, J. Elser, P. Jaiswal, P. Gupta, P. Jaiswal, S. Naithani, M. Lera-Ramirez, K. Rutherford, V. Wood, J.L. De Pons, M.R. Dwinell, G.T. Hayman, M.L. Kaldunski, A.E. Kwitek, S.J. F. Laulederkind, M.A. Tutaj, M. Vedi, S.J. Wang, P. D'Eustachio, L. Aimo, K. Axelsen, A. Bridge, N. Hyka-Nouspikel, A. Morgat, S.A. Aleksander, J.M. Cherry, S.R. Engel, K. Karra, S.R. Miyasato, R.S. Nash, M.S. Skrzypek, S. Weng, E.D. Wong, E. Bakker, T.Z. Berardini, L. Reiser, A. Auchincloss, K. Axelsen, G. Argoud-Puy, M. C. Blatter, E. Boutet, L. Breuza, A. Bridge, C. Casals-Casas, E. Coudert, A. Estreicher, M. Livia Famiglietti, M. Feuermann, A. Gos, N. Gruaz-Gumowski, C. Hulo, N. Hyka-Nouspikel, F. Jungo, P. Le Mercier, D. Lieberherr, P. Masson, A. Morgat, I. Pedruzzi, L. Pourcel, S. Poux, C. Rivoire, S. Sundaram, A. Bateman, E. Bowler-Barnett, A.J.H. Bye, P. Denny, A. Ignatchenko, R. Ishtiaq, A. Lock, Y. Lussi, M. Magrane, M.J. Martin, S. Orchard, P. Raposo, E. Speretta, N. Tyagi, K. Warner, R. Zaru, A.D. Diehl, R. Lee, J. Chan, S. Diamantakis, D. Raciti, M. Zarowiecki, M. Fisher, C. James-Zorn, V. Ponferrada, A. Zorn, S. Ramachandran, L. Ruzicka, M. Westerfield, The Gene Ontology knowledgebase in 2023, Genetics 224 (1) (2023).

[39] S. La Monica, D. Madeddu, M. Tiseo, V. Vivo, M. Galetti, D. Cretella, M. Bonelli, C. Fumarola, A. Cavazzoni, A. Falco, A. Gervasi, C.A. Lagrasta, N. Naldi, E. Barocelli, A. Ardizzoni, F. Quaini, P.G. Petronini, R. Alfieri, Combination of Gefitinib and Pemetrexed Prevents the Acquisition of TKI Resistance in NSCLC Cell Lines Carrying EGFR-Activating Mutation, J. Thorac. Oncol. 11 (7) (2016) 1051–1063.
[40] G.Y. Di Veroli, C. Fornari, D. Wang, S. Mollard, J.L. Bramhall, F.M. Richards, D. I. Jodrell, Combenefit: an interactive platform for the analysis and visualization of drug combinations, Bioinformatics 32 (18) (2016) 2866–2868.
[41] S. Musa, N. Amara, A. Selawi, J. Wang, C. Marchini, A. Agbarya, J. Mahajna, Overcoming Chemoresistance in Cancer: The Promise of Crizotinib, Cancers (Basel) 16(13) (2024).
[42] S.L. Organ, M.S. Tsao, An overview of the c-MET signaling pathway, Ther Adv Med Oncol 3 (1 Suppl) (2011) S7–S19.
[43] W.Z. Qiu, H.B. Zhang, W.X. Xia, L.R. Ke, J. Yang, Y.H. Yu, H. Liang, X.J. Huang, G. Y. Liu, W.Z. Li, Y.Q. Xiang, T.B. Kang, X. Guo, X. Lv, The CXCL5/CXCR2 axis contributes to the epithelial-mesenchymal transition of nasopharyngeal carcinoma cells by activating ERK/GSK-3beta/snail signalling, J. Exp. Clin. Cancer Res. 37 (1) (2018) 85.
[44] L. Chen, X.W. Pan, H. Huang, Y. Gao, Q.W. Yang, L.H. Wang, X.G. Cui, D.F. Xu, Epithelial-mesenchymal transition induced by GRO-alpha-CXCR2 promotes bladder cancer recurrence after intravesical chemotherapy, Oncotarget 8 (28) (2017) 45274–45285.
[45] H.M. Jeon, J. Lee, MET: roles in epithelial-mesenchymal transition and cancer stemness, Ann Transl Med 5 (1) (2017) 5.
[46] M. Stadler, M. Scherzer, S. Walter, S. Holzner, K. Pudelko, A. Riedl, C. Unger, N. Kramer, B. Weil, J. Neesen, M. Hengstschlager, H. Dolznig, Exclusion from spheroid formation identifies loss of essential cell-cell adhesion molecules in colon cancer cells, Sci. Rep. 8 (1) (2018) 1151.
[47] S.J. Han, S. Kwon, K.S. Kim, Challenges of applying multicellular tumor spheroids in preclinical phase, Cancer Cell Int. 21 (1) (2021) 152.
[48] A. Frille, M. Boeschen, H. Wirtz, M. Stiller, H. Blaker, M. von Laffert, TP53 co-mutations in advanced lung adenocarcinoma: comparative bioinformatic analyses suggest ambivalent character on overall survival alongside KRAS, STK11 and KEAP1 mutations, Front. Oncol. 14 (2024) 1357583.
[49] F. Skoulidis, B.T. Li, A.J. de Langen, D.S. Hong, H. Lena, J. Wolf, G.K. Dy, A. Curioni Fontecedro, P. Tomasini, V. Velcheti, A.J. van der Wekken, C. Dooms, L. Paz-Ares Rodriguez, G. Mountzios, A. Sacher, E. Nadal, S. Couraud, S.W. Kim, K. O'Byrne, D. Rocco, R. Toyozawa, I. Chmielewska, C.R. Lindsay, A. Hindoyan, L. Mukundan, T. Wilmanski, A. Anderson, C. Ardito-Abraham, A. Pati, A. Reddy, B. Mehta, M. Schuler, Molecular determinants of sotorasib clinical efficacy in KRAS (G12C)-mutated non-small-cell lung cancer, Nat. Med. (2025).
[50] S. Yu, M. Yi, L. Xu, S. Qin, A. Li, K. Wu, CXCL1 as an Unfavorable Prognosis factor Negatively Regulated by DACH1 in Non-small Cell Lung Cancer, Front. Oncol. 9 (2019) 1515.
[51] D.W. Edwardson, J. Boudreau, J. Mapletoft, C. Lanner, A.T. Kovala, A. M. Parissenti, Inflammatory cytokine production in tumor cells upon chemotherapy drug exposure or upon selection for drug resistance, PLoS One 12 (9) (2017) e0183662.
[52] G.E. Wood, H. Hockings, D.M. Hilton, S. Kermorgant, The role of MET in chemotherapy resistance, Oncogene 40 (11) (2021) 1927–1941.
[53] L.R. Richard Riedel, Malte Verheyen, Felix John, Heather Scharpenseel, Lucia Nogova, Sebastian Michels, Rieke N. Fischer, Anna Eisert, Carolin Jakob, Emanuel Niesen, Jana Fassunke, Janna Siemanowski-Hrach, Carina Heydt, Anne Bunck, Udo Siebolts, Sabine Merkelbach-Bruse, Reinhard Buettner, Jürgen Wolf, Matthias Scheffler, Brief Report: MET driven resistance to sotorasib in KRAS G12C-mutant Non-small cell lung cancer and response to combined KRAS and MET inhibition, JTO Clinical and Research Reports, 2025.
[54] R. Rosell, E. Jantus-Lewintre, P. Cao, X. Cai, B. Xing, M. Ito, J.L. Gomez-Vazquez, M. Marco-Jordan, S. Calabuig-Farinas, A.F. Cardona, J. Codony-Servat, J. Gonzalez, K. Valencia-Clua, A. Aguilar, C. Pedraz-Valdunciel, Z. Dantes, A. Jain, S. Chandan, M.A. Molina-Vila, O. Arrieta, M. Ferrero, C. Camps, M. Gonzalez-Cao, KRAS-mutant non-small cell lung cancer (NSCLC) therapy based on tepotinib and omeprazole combination, Cell Commun. Signal 22 (1) (2024) 324.
[55] Y. Feng, E.C. Minca, C. Lanigan, A. Liu, W. Zhang, L. Yin, N.A. Pennell, C. Farver, R. Tubbs, P.C. Ma, High MET receptor expression but not gene amplification in ALK 2p23 rearrangement positive non-small-cell lung cancer, J. Thorac. Oncol. 9 (5) (2014) 646–653.
[56] L. Song, L. Zhang, Y. Zhou, X. Shao, Y. Xu, D. Pei, Q. Wang, ORP5 promotes tumor metastasis via stabilizing c-Met in renal cell carcinoma, Cell Death Discov 8 (1) (2022) 219.
[57] Y. Adachi, K. Ito, Y. Hayashi, R. Kimura, T.Z. Tan, R. Yamaguchi, H. Ebi, Epithelial-to-Mesenchymal transition is a Cause of both Intrinsic and acquired Resistance to KRAS G12C Inhibitor in KRAS G12C-mutant Non-Small Cell Lung Cancer, Clin. Cancer Res. 26 (22) (2020) 5962–5973.
[58] Z. Pan, Y. Qian, Y. Wang, T. Zhang, X. Song, H. Ding, R. Li, Y. Zhang, Z. Wang, H. Wang, W. Xia, L. Wei, L. Xu, G. Dong, F. Jiang, STAT3 Inhibition Prevents Adaptive Resistance and Augments NK Cell Cytotoxicity to KRAS(G12C) Inhibitors in Nonsmall Cell Lung Cancer, Cancer Sci. 116 (5) (2025) 1375–1391.
[59] Z.Y. Zheng, M.Y. Chu, W. Lin, Y.Q. Zheng, X.E. Xu, Y. Chen, L.D. Liao, Z.Y. Wu, S. H. Wang, E.M. Li, L.Y. Xu, Blocking STAT3 signaling augments MEK/ERK inhibitor efficacy in esophageal squamous cell carcinoma, Cell Death Dis. 13 (5) (2022) 496.
[60] P. Granado-Martinez, S. Garcia-Ortega, E. Gonzalez-Sanchez, K. McGrail, R. Selgas, J. Grueso, R. Gil, N. Naldaiz-Gastesi, A.C. Rhodes, J. Hernandez-Losa, B. Ferrer, F. Canals, J. Villanueva, O. Mendez, S. Espinosa-Gil, J.M. Lizcano, E. Munoz-Couselo, V. Garcia-Patos, J.A. Recio, STK11 (LKB1) missense somatic mutant isoforms promote tumor growth, motility and inflammation, Commun. Biol. 3 (1) (2020) 366.
[61] D.B. Mahat, H. Kumra, S.A. Castro, E. Metcalf, K. Nguyen, R. Morisue, W.W. Ho, I. Chen, B. Sullivan, L.H. Yim, A. Singh, J. Fu, S.K. Waterton, Y.C. Cheng, E. Moiso, V. P. Chauhan, H.M. Silva, S. Spranger, R.K. Jain, P.A. Sharp, Mutant p53 exploits enhancers to elevate immunosuppressive chemokine expression and impair immune checkpoint inhibitors in pancreatic cancer, Immunity 58(7) (2025) 1688-1705 e9.
[62] Z. Zhang, R. Hao, Q. Guo, S. Zhang, X. Wang, TP53 Mutation Infers a Poor Prognosis and is Correlated to Immunocytes Infiltration in Breast Cancer, Front. Cell Dev. Biol. 9 (2021) 759154.
[63] I. Canadas, F. Rojo, A. Taus, O. Arpi, M. Arumi-Uria, L. Pijuan, S. Menendez, S. Zazo, M. Domine, M. Salido, S. Mojal, A. Garcia de Herreros, A. Rovira, J. Albanell, E. Arriola, Targeting epithelial-to-mesenchymal transition with Met inhibitors reverts chemoresistance in small cell lung cancer, Clin. Cancer Res. 20 (4) (2014) 938–950.
[64] S.L. Zhou, Z.J. Zhou, Z.Q. Hu, X. Li, X.W. Huang, Z. Wang, J. Fan, Z. Dai, J. Zhou, CXCR2/CXCL5 axis contributes to epithelial-mesenchymal transition of HCC cells through activating PI3K/Akt/GSK-3beta/Snail signaling, Cancer Lett. 358 (2) (2015) 124–135.
[65] L. Wang, J. Gao, S. Zheng, Z. Luo, Z. Xu, H. Che, Z. Wang, CXCR2/Snail-1-Induced Epithelial-Mesenchymal transition in the Formation and Progression of RCC with Inferior Vena Cava Tumour Thrombus, Arch. Esp. Urol. 77 (3) (2024) 292–302.